DYNAMIC MODELING OF A MAGNETIC LEVITATION SYSTEM

''MAGNEETILISE LEVITATSIOONI SÜSTEEMI DÜNAAMILINE MODELLEERIMINE''

MASTER THESIS

Student:	Malith Bhanuka Unamboowe
Student code:	194529 MAHM
Supervisor:	Hossein Alimohammadi, Junior Researcher

Co-Supervisors: Aleksei Tepljakov, Senior Researcher
Viktor Rjabtšikov, Junior Researcher

Tallinn 2021

AUTHOR'S DECLARATION

Hereby I declare, that I have written this thesis independently.

No academic degree has been applied for based on this material. All works, major viewpoints and data of the other authors used in this thesis have been referenced.

"21" December 2021

Author: ....
    /signature /

Thesis is in accordance with terms and requirements

"......." .... 20….

Supervisor: …........................
    /signature/

Accepted for defence

"......."....................20… .

Chairman of theses defence commission: ....
    /name and signature/

Non-exclusive Licence for Publication and Reproduction of GraduationTthesis[1]

I, Ekanayake Rajakaruna Wasala Mudiyanselage Malith Bhanuka Unamboowe (1994-09-06)

1. grant Tallinn University of Technology (TalTech) a non-exclusive license for my thesis "Dynamic modeling of a magnetic levitation system"

supervised by Mr. Hossein Alimohammadi

1.1 reproduced for the purposes of preservation and electronic publication, incl. to be entered in the digital collection of TalTech library until expiry of the term of copyright;

1.2 published via the web of TalTech, incl. to be entered in the digital collection of TalTech library until expiry of the term of copyright.

1.3 I am aware that the author also retains the rights specified in clause 1 of this license.

2. I confirm that granting the non-exclusive license does not infringe third persons' intellectual property rights, the rights arising from the Personal Data Protection Act or rights arising from other legislation.

---

[1] *Non-exclusive Licence for Publication and Reproduction of Graduation Thesis is not valid during the validity period of restriction on access, except the university`s right to reproduce the thesis only for preservation purposes.*

_____ (*signature*)

21/12/2021 (*date*)

Department of Electrical Power Engineering and Mechatronics
THESIS TASK

Student: Ekanayake Rajakaruna Wasala Mudiyanselage Malith Bhanuka Unamboowe, 194529MAHM

Study programme MAHM02/18-Mechatronics

main speciality: Mechatronics

Supervisor(s): Junior Researcher, Hossein Alimohammadi, (position, name, phone)

Co-Supervisors: Senior Researcher, Aleksei Teplijakov

                Junior Researcher, Viktor Rjabtšikov

Thesis topic:

(in English)   Dynamic modelling of a magnetic levitation system

(in Estonian) Magneetilise levitatsioooni süsteemi dünaamiline modeleerimine

Thesis main objectives:

1. Linear models which are PD is not suitable for highly nonlinear systems and need a better alternative such as a Fuzzy logic controller.

2. Implemented and developed alternative controllers should have a much quicker response rate since the system is unstable, to begin with.

3. New FLC should have a lower steady-state error compared to the original PD controller.

Thesis tasks and time schedule:

No	Task description	Deadline
1.	Data acquisition for the PD controller.	15.10.2021
2.	Development of a Fuzzy logic controller.	01.11.2021
3.	Comparison of simulation data for both controllers	30.11.2021
4.	Running the Fuzzy logic controller in the real system	30.11.2021
5.	Thesis defence	19.01.2022

Language: English **Deadline for submission of thesis:** 21" December 2021

Student: Malith Bhanuka Unamboowe   "......."…………......................2021
                                                      /signature/

Supervisor: Hossein Alimohammadi   "......."................................2021
                                                      /signature/

Co-Supervisors: Aleksei Teplijakov   "......."................................2021
                                                      /signature/

Viktor Rjabtšikov   "......."................................2021

                                     /signature/

Head of study programme: Anton Rassõlkin   "......."................................2021

                                     /signature/

Terms of thesis closed defence and/or restricted access conditions to be formulated on the reverse side

TABLE OF CONTENTS

PREFACE

The Master Thesis topic of Dynamic Modelling of a magnetic levitation system was initially proposed by Researcher Hossein Alimohammadi from Tallinn University of Technology. The control system Magnetic Levitation System for two electromagnets or MLS2EM is currently located and the experiment was conducted in the control laboratory at Tallinn University of Technology.

The main focus point of the thesis was to implement a better alternative controller for the PD controller which was initially in the system. The original system including the PD controller was created by the Polish company INTECO and the whole experiment is quite challenging and interesting, to begin with. The discussed approach was to create a Fuzzy logic controller to replace the PD controller by maintaining the same result outcome with a much quicker response time and accuracy without any overshooting or undershooting.

LIST OF FIGURES

LIST OF TABLES

ABBREVIATIONS

MLS – Magnetic Levitation System

MLS2EM - Magnetic Levitation System with two electromotive force

EM - Electro Magnetic

EMF - Electro-Motive Forces

PWM – Pulse Width Modulation

FLC - Fuzzy Logic Controller

PID - Proportional Integral Derivative

PD - Proportional Derivative

SMC – Sliding Mode Control

PI – Proportional Integtal

EMS – Electro Magnetic Suspension

GUI – Graphical User Interface

I/O – Input/Output

1. INTRODUCTION

In recent times there has been a lot of research and development in the magnetic levitation field. Currently, the implementation of magnetic levitation systems or MLS is very narrow in the application field. One of the applications of magnetic levitation is trains that will be running under this phenomenon which are not very abundant due to the high cost and requirement of high resources. Originally this technology was engineered in Germany and currently only one line operating in China (Shanghai Maglev).

Magnetic levitation system 2EM (MLS2EM) by Inteco is a custom assembled laboratory system with full control access towards the experiments. The control system is to deal with the metallic sphere position control of a MLS, which is an intricate and highly nonlinear system [1]. The proposed control system in [1] consists of an adaptive PID controller and a fuzzy compensation controller.

The electromagnetic levitation represents a classical control subject matter for which various solutions were developed. Many of them converged on a voltage-control feedback linearization [2][3]. In this specific task, we will use MATLAB and Simulink to emulate the experiment. Simply we will use the upper magnet to equalize the gravitational force by the sphere. The 2nd magnet will act as a disturbance to the whole unit. The resultant of this MLS can apply in a robust controller design. There is not much space to manoeuvre the sphere since it is operated in a confined space. Such MLS's with small operating ranges have been proposed by various researchers [4].

In the MLS2EM when the sphere is at its equilibrium position (when no external force is acting in the metallic sphere) the resultant of all the forces which are acting upon the magnet is zero. In the experiment, two magnets EM1 and EM2 were used to balance the sphere between the gap x_1 [5]. Considering the physical model, it can be described as an object in the air without contact with the object, by using electromagnetic phenomena. The resultant will be a mechanical system that is in three force equilibrium and all occurring forces are parallel to each other. Additionally, two force equilibrium also can be achieved by cutting off the lower magnet from the operation. There is already a system built similar to this without the lower magnet. The figure for the physical setup for the experiment is shown in Figure 1.

Figure 1. Experimental setup with the metallic sphere on the resting platform

As shown in Figure 1, both EM1 and EM 2 are mounted in the given yellow metallic frame as in the upper and lower frame of the fixture. Two-position sensors are mounted towards the side of the frame. The screw which is situated in the bottom of the lower EM2 allows changing the platform height where the ball will be resting before the simulation run.

2. LITERATURE REVIEW

2.1 Background Research of MLS

Magnetic Levitation system or MLS is a highly non-linear control system with positioning control using two electromagnets [6]. Several types of models have been implied and stated for similar projects and in many types of research, each of them has a different vantage view of the problem and solving it. In the MLS2EM, a mathematical model will be used with the use of Simulink to emulate and conduct the experiment.

In the given system it consists of two electromagnets (EM1 – upper and EM2 – lower), metal sphere, position sensors to detect the sphere location, and relevant drivers and software to implement the experiment [6]. In this specific model, we will be using PD control instead of the PID control to operate and conduct the experiment. In the given experiment we can get a setpoint using only EM1 electro-magnet but in this specific case, we will deactivate EM2 and later it can be used as an external disturbance to determine the setpoint change due to acting upon it. But when it comes to highly non-linear systems PD controller is not suitable and need to consider different methods.

Although MLS2EM is mostly based on theoretical work there is a lot of application research has been done regarding MLS. MLS implementation regarding wireless charging platform and this was done using a PWM signal to adjust the platform height due to changes in the coil current [11]. This allows the receiver to have a 10mm gap from the wireless transmitter [11]. Application of MLS can vary from simple household items to industrialized applications such as MAGLEV trains. Since MAGLEV is an environmentally friendly transportation method with such key advantage factors as low noise, high efficiency, comparatively low maintenance costs, a very comfortable ride due to lack of ground friction [12]. In this concept, both the levitation magnets and the guidance magnets are fixed in a single rail [12]. When placing the guidance EM and the levitation EM close to each other magnetic coupling effect will take on action [13]. This coupling effect will only depend on the current direction of the guidance EM [13].

Even though MLS2EM position sensors determine the location of the sphere and adjust the setpoint based on that some research experiments will use image processing to do the same task. When the steel sphere was displaced by its setpoint, the distance between EM and the sphere will adjust according to that output voltage of the sensor changes, the levitation control circuit will generate a signal which will resultant in adjusting the current in EM through the control signal [14].

Although conventionally when considering a controller such as a PID is the basic design step for a well-defined model that can be controlled or developed [15]. But all the assumptions and simplifications that will consider related to simplified modelling the resultant will be a weaker control. When modelling the systems is too hard to accomplish or modify, the Fuzzy logic controllers can be used as alternatives [15]. Fuzzy control can be explained as a binary logic that has been modified so it can handle intermediate values between 0 (totally false) and 1 (totally true) [16]. Usually, fuzzy logic control will be used when the analysis is too complicated for an alternative model or controller [16]. Furthermore, spheres were made out of EM's for levitating the rotors of an induction motor to obtain a multi-layer spherical metal shell [17].

Filter-based tracking was used in MLS as an alternative for position sensors and image processing and it is based on Lagrange- Maxwell equation the non-linear model for the MLS was achieved [18]. There is research work where state space analysis will be used to optimize the range parameters such as the MLS ED-4810 [19]. State-space equations are used to describe a system in the time-domain using first-order differential equations [19]. The goal of using the state-space system is to linearize a non-linear system [19].

Another approach for MLS is the sliding control model which does not require an accurate model, it has key advantages such as a really fast response rate and no external disturbance, and no sensitivity to parameters are just a few of them [20]. Not only does SMC have a good steady-state suspension for the magnetic levitation ball it has a very accurate tracking performance as well [20].

There have been some improvements in the suspension systems for MAGLEV trains an adaptive neural-fuzzy SMC is presented consisting of the sliding surface, neural-fuzzy switch, and an adaptive-fuzzy estimator [21]. But with the rapid improvements of control theory, there are different types of control modes for MLS which is becoming harder to obtain better control effects resulting in complex algorithms [21].

Regarding from modelling perspective for an MLS system usually, it is consists of a mechanical system and as well an electrical system [22]. These two systems will act correlatively to each other by manoeuvring the sphere using a mechanical system which will be controlled by the electrical system [22]. The resultant of the mechanical capability is highly depends on the amount of current flowing through the EM coil. Considering the equilibrium in this Newtonian model acceleration of the metallic sphere is directly proportional to the square of the current flow.

There can be external factors that will be directly impacted the metallic sphere rather than the EM coil. These forces can be external as a physical force such as wind, heat or

other impactful forces which will give a manipulated result from the original. When considering air resistance or formally known as drag force is proportional to the square of the velocity and would also be proportional to the density of the fluid [23]. If the experiment was done in a laboratory environment this density would be changed to air density in the given situation.

When considering air resistance, the Reynolds number is a key feature to determine the drag coefficient. Depending on the Reynolds number one can determine whether the sphere will be accounted for lamina flow or turbulent flow. The main downside is that the drag coefficient cannot be illustrated in an analytical form that will have a massive range of particle Reynolds numbers, the flowing dynamics during the process is highly advanced [24].

Relatively to air resistance heat or thermal plays a significant part in electromagnetic suspension (EMS) in MLS. The heat increment will cause to change the resistance on the EM and therefore need to transmit a sufficient amount of current to maintain the air gap between the vehicle and guided railway [25].

2.2 Additional research

Although several other approaches and methods are also being used to solve similar MLS problems. Mainly using electromagnetic modelling point of view which can be classified by Kirchhoff's voltage law for the specific problem [8].

$$u(t) = V_R + V_L = iR + \frac{dL(x)i}{dt} \tag{2.1}$$

Where

      u- applied voltage, V,

      i - current going through an electromagnet coil, A,

      R- resistance of the coil, Ω,

      L- inductance of the coil, H,

      V_R- Voltage drop of the resistor, V,

      V_L- Voltage drop of the inductor, V.

In this model, it's strictly done by electromagnetic modelling which will be helpful when calculating flux densities and ranges. Other than the theoretical point of view, this electromagnetic modelling cannot be expanded towards the application side as much as a mathematical model.

When it comes to electromagnetic induction of a voltage coil due to movement of a rigid magnet or as defined electromagnetic generation permanent magnets were used to generate electricity [9]. In this case, we need to take EMF into account. Then the maglev component can move freely between the two magnets resulting in an electromagnetic generation.

In addition to these, the tensor product-based model was proposed since it can be applied for both linear and non-linear systems and can directly apply to transformation systems [10]. This is important since the non-linear part of the model can be directly used for MLS [10]. Tensor based models are mainly used for multi-input and multi-output control systems which requires numerical analysis for each parameter [27]. The main modelling process for tensor product based is linear-time variant systems and quasilinear parameter-varying models which use state-space systems and matrix representation to represent parameters [27].

2.3 Literature Review Conclusion

- In conclusion lot of theoretical work has been done regarding magnetic levitation systems. There are also practical works are done as well up to some extent. But long term industrial experimental projects such as Maglev rail and magnetically propelled vehicles are very rare to find in the operational stage and most of them are still on the developing stage due to high costs.
- Most theoretical research regarding magnetic levitation systems is done through mathematical modelling or FLC since it's the easiest and the application capability is high compared to a mechanical model or an electromagnetic model.

- Since when considering the flux patterns around the sphere mathematical model is easily applicable for the expansion for that specific area because the setpoints are changing and the flux is changing as well and due to this results in a highly non-linear and discrete system.

- Most of the researches have down comings as well such as mathematical models being too complicated in a way requiring too much-complicated algorithms. The models need some modification to implement more efficiently.

- Most of the systems were proven for an ideal system that hasn't considered surrounding factors such as heat, wind and resistive other forces which can have an external impact on the whole system. Even though most of these practicals

were done at the laboratory level most of the external factors are kept to a minimum.

2.4 Project Objectives

The main objectives of the research are stated as below,

- Modify the controller so it will be easier to determine and adjust the set point of the metallic sphere.
- Applying a modified mathematical model and FLC to improve the control functionalities and get a more robust system than the initial system.
- Change the FLC so it will be a better alternative and quicker responsive than the PD controller.
- Minimize the steady-state offset from the desired position.

3. METHOD AND MODELLING

This chapter identifies which characteristics and problems which were occurred during the initial part of the original experiment and what improvement methods were done to avoid those problems. The main focus objective is to control and manipulate the values of Proportional, Derivative and Steady-state values and how the control system behaves according to the given changes. As an additional part of the comparison, an inbuilt PID controller was selected on Simulink and tried to tune as same as the PD controller which was created by Inteco. But tuning the PID controller was much more time consuming and difficult. When the PID was created to be quick responsive lot of overshooting and undershooting can be seen. This is a negative impact considering from a control perspective.

3.1 Original model and characteristics

The original model mainly consists of two preliminary parts which will support the system. One is the PD controller which will control the whole system and a mathematical model which is represented by the Newtonian method to balance the sphere. In the initial model, it appears as a closed-loop system which will take the position as the feedback. The main Simulink setup at its initial state is illustrated in Figure 2.
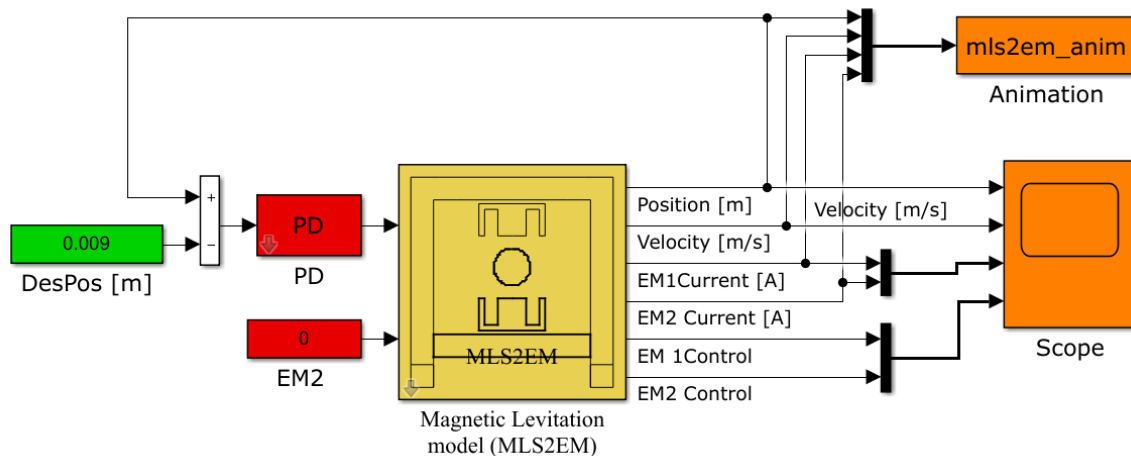
Figure 2. Simulink setup with PD controller connected to the mathematical model

Figure 2, represents the Simulink model for the control system. The system can be divided into four separate due to functionality to the system. These four parts can be described as setpoint parameter (green), controllers (red), mathematical model (yellow) and visualization (orange). The green function block denotes the given setpoint for the control system. And from the difference of the actual position value from the feedback,

the resultant error was given to the PD controller which is represented in the red function block. For the initial condition, EM2 was set to 0 as shown in Figure 2 and the output of the PD controller was connected to EM1 of the mathematical model.

To observe the changes in parameters, outputs of the mathematical model such as position (m), velocity (m·s^{-1}), current (A) and control was given to a visual scope. All these parameters were given to the animation block which can be seen in Figure 2 for a visual representation of the sphere on an animated screen that is updating in each sample time interval.

3.1.1 Mathematical model for the control system

The physical representation of the mathematical model can be shown as a free body diagram for forces as in Figure 3 which will be using three forces to equalize the metallic sphere.
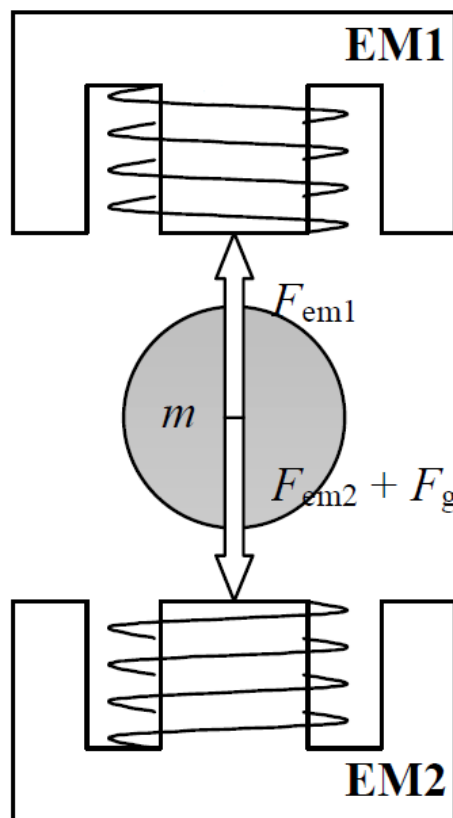
Figure 3. MLS2EM free body diagram for acting forces [5]

Basically to solve the physical problem basic laws of physics needed to be taken into account. The physical equilibrium happens when [5],

$$F_{em1} = F_{em2} + Fg \qquad (3.1)$$

Where

F_{em1} - electromagnetic force due to EM1, N,

F_{em2} - electromagnetic force due to EM2, N,

Fg - gravitational force due to sphere weight, N.

The mathematical model was stated as a state-space representation and the given equations are stated as below [7].

$$\frac{dx_1}{dt} = x_2 \qquad (3.2)$$

$$\frac{dx_2}{dt} = \frac{-F_{em1}}{m} + g + \frac{F_{em2}}{m} \qquad (3.3)$$

$$\frac{dx_3}{dt} = \frac{(k_i u_1 + C_i - x_3)}{f_i(x_1)} \qquad (3.4)$$

$$\frac{dx_4}{dt} = \frac{(k_i u_2 + C_i - x_4)}{f_i(x_d - x_1)} \qquad (3.5)$$

where

$$F_{em1} = x_3^2 \left(\frac{F_{emp1}}{F_{emp2}}\right) e^{\left(\frac{-x_1}{F_{emp2}}\right)} \ ,$$

$$F_{em2} = x_4^2 \left(\frac{F_{emp1}}{F_{emp2}}\right) e^{\left(\frac{x_1 - x_d}{F_{emp2}}\right)} ,$$

$$F_i(x_1) = \frac{f_i P_1}{f_i P_2} e^{\frac{-x_1}{f_i P_i}} \qquad \text{for both actuators}$$

where

$X_1 \in [0 , 0.016]$,

$X_2 \in [\Re]$,

$X_3 \in [i_{min}, 2.38]$,

$X_4 \in [i_{min}, 2.38]$,

$u_1 \in [u_{MIN}, 1]$,

$u_2 \in [u_{MIN}, 1]$.

As seen from the equations two factors will determine the intensity of the EMF; the sphere distance gap between the electromagnet and the current running through the electromagnetic coil [7]. The parameters of the above equations are represented in Table 3.1 given below [7].

Table 3.1 Parameters for the non-linear state-space equations [7]

Parameters	Values	Units
m	$5,71 \cdot 10^{-2}$	[Kg]
g	9,81	[m/s^2]
F_{em1}, F_{em2}	Functions of x_1 and x_3	[N]
F_{emp1}	$1,7521 \cdot 10^{-2}$	[H]
F_{emp2}	$5,8231 \cdot 10^{-3}$	[m]
$f_i(x_i)$	Function of x_1	[1/s]
f_iP_1	$1,4142 \cdot 10^{-4}$	[m/s]
f_iP_2	$4,5626 \cdot 10^{-3}$	[m]
C_i	$2,43 \cdot 10^{-2}$	[A]
K_i	2,5165	[A]
x_d	Distance between electromagnets minus ball diameter (Can be modified by the user)	[m]
i_{min}	$3,884 \cdot 10^{-2}$	[A]
u_{MIN}	$4,98 \cdot 10^{-3}$	

Although Simulink representation of the mathematical model consists of two current models and two force models for each magnet to function the system. In this original model, we are handling a third-order dynamical system. From the resultant forces, the resultant acceleration of the sphere was calculated and then it was run through two integrators to get real-time velocity and position for the sphere respectfully. Since the position is the feedback for this control system saturation limits were given as $2 \cdot 10^{-2}$ m (upper saturation limit) and $1 \cdot 10^{-4}$ m (lower saturation limit).

The initial starting position can be within this range so it can reach the desired position of $9 \cdot 10^{-3}$ m from both the upper limit and the lower limit. Other initial state parameters also can be changed according to the control system.

Table 3.2 Initial state parameters of the control system by default

Initial state	Value	Units
Position	$9 \cdot 10^{-3}$	m
Velocity	0	$m \cdot s^{-1}$
EM1 current	0,9	A
EM2 current	$4 \cdot 10^{-2}$	A

The mathematical model for the original control system in Simulink is shown in Figure 4 below.
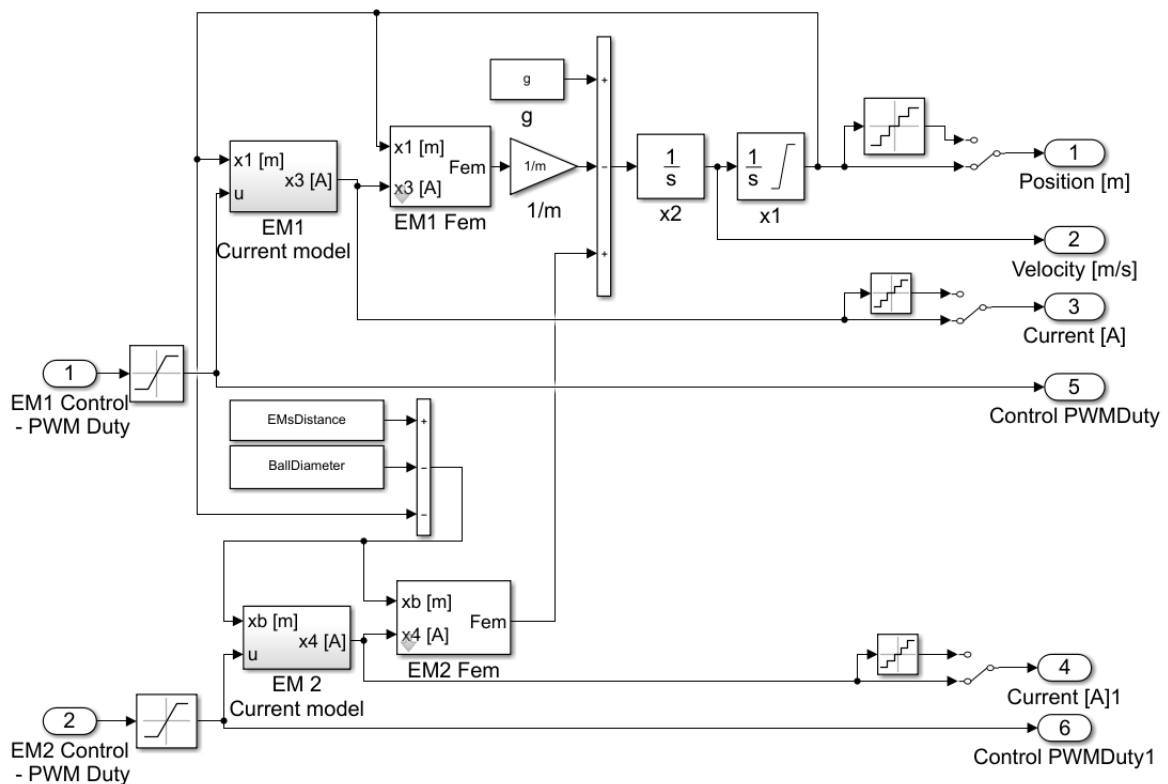
Figure 4. Simulink representation of the mathematical model block

The mathematical model was given two inputs for each magnet's PWM control and six outputs (position, velocity, EM1current, EM1control, EM2current, EM2control) were taken out from the mathematical model to observe the control system. As shown in Figure 4, resultant acceleration was obtained by adding the acceleration due to EM2 and gravitational impact and then subtracting by the acceleration due to EM1. The resultant acceleration was run through two integrators x2 and x1 respectively to get the position parameter which will be the feedback of the control system.

3.1.2 PD controller

The main controller of the control system is a PD controller which is taking the position offset error as the input for the proportional variable and changes of this error component as the derivative part. So initially to stabilize the control system two parameters needed to take into consideration which is error and change of error. Also, different parameters can be taken into consideration as well such as real-time position and change of position (velocity) of the system.

Initial parameters were given for proportional gain constant (K_p), proportional derivative constant (K_d) and steady-state control (u0) so the PD controller will be functioning accordingly. The given values are stated in Table 3.3.

Table 3.3 Initial parameters for PD controller setup [7]

Parameter	Value
K_p	55
K_d	5
u0	0,3617

For the whole part of this experiment, sample time was kept at $1 \cdot 10^{-3}$ seconds to observe the results in an accurate environment. Saturation limits were given by default for the PD controller as 0 (lower saturation limit) and 1 (upper saturation limit). The Simulink representation of the PD controller is stated in Figure 5 as given below.

Figure 5. Simulink representation for the PD controller subsystem

Figure 5 shows K_p as proportional gain, K_d as derivative gain and u0 as the steady-state parameter. All three variables were given to an addition block and output was taken through a saturation box with mentioned 0 and 1 saturation limits.

To test the PD controller impact on the control system it requires closely observing how I/O characteristics will behave from the start of the simulation until it comes to the stabilized level. To gather the I/O data, separate scopes needed to be given for each of the parameters and the taken data were added to the workspace in the matrix form. Next, these data sets were used to plot the graph of position error vs PD output. To simplify the graphing process a Matlab code was used to plot the graph and similar code with minor changes were used to plot all the other graphs as well.

When the initial starting point of the sphere is set for $2 \cdot 10^{-4}$ m and the experiment was run to observe the I/O behaviour of the PD controller. From the shown image in Figure 6 behaviour between error vs PD, output was plotted.
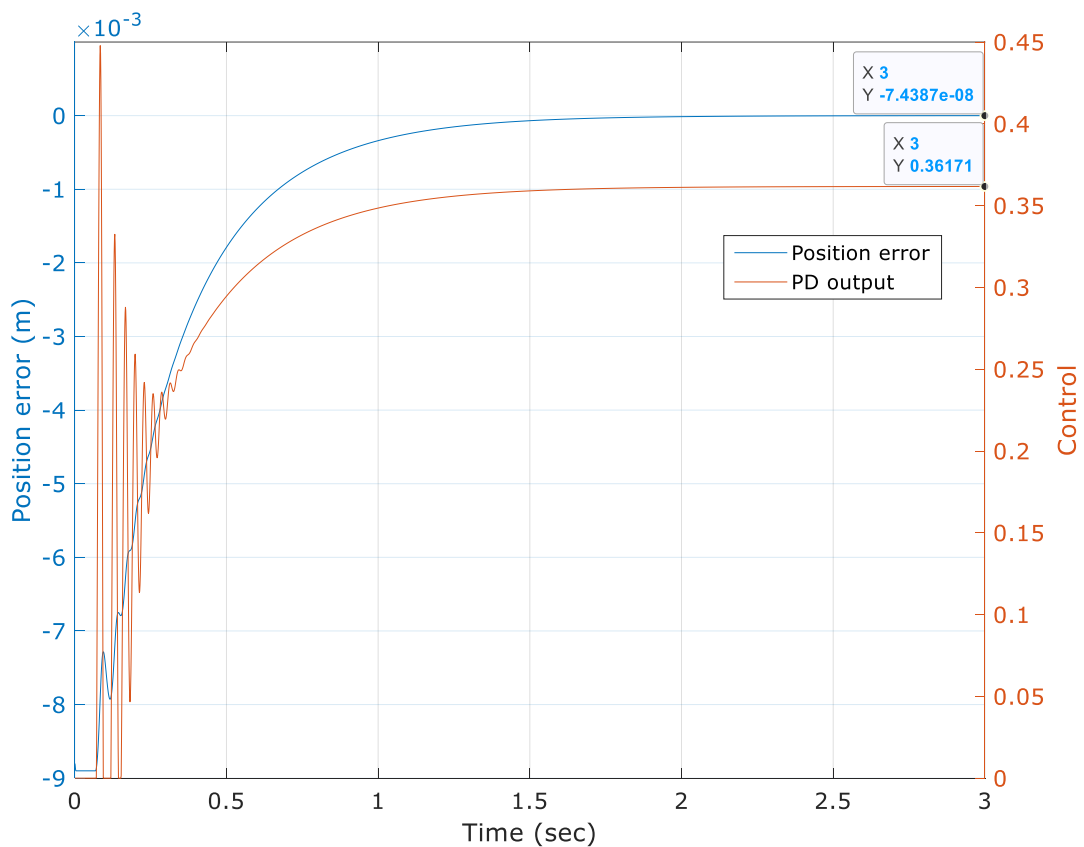
Figure 6. Position error vs PD output

As seen in the graph in Figure 6, after some overshooting the PD controller output stabilize on the value of 0,3617 and will continue to maintain this until the time reaches infinity.

The initial starting point was $2 \cdot 10^{-4}$ m which is nearly close to zero making a small negative position error at the start since the desired position was $9 \cdot 10^{-3}$ m. During this three-second run time error is closing on zero as the result of the PD control output giving an equalized control system as the sphere reaches the given desired position of $9 \cdot 10^{-3}$ m. All these distances were calculated from the lower surface of the upper EM to the metallic sphere.

3.2 Data acquisition for the control system

Before running the simulation the distance between electromagnets were kept at $7.5 \cdot 10^{-2}$ m and the ball with a diameter of $6 \cdot 10^{-2}$ m was considered. When reaching the equilibrium position the desired position should be equal to the actual position which is $9 \cdot 10^{-3}$ m and velocity at that same time needed to be zero. Because if velocity is either negative or positive it would not stay in the desired position and will cause a negative or positive error. This is the reason that the control system of MLS cannot be controlled by a just proportional controller and need the additional derivative part.

The simulation was run for ten seconds with the initial starting point is set to $2 \cdot 10^{-4}$ m. After two second runtime, the simulation is reaching marginally close to the desired position level of $9 \cdot 10^{-3}$ m. Below graph in Figure 7 shows the position output for the ten second run time frame.
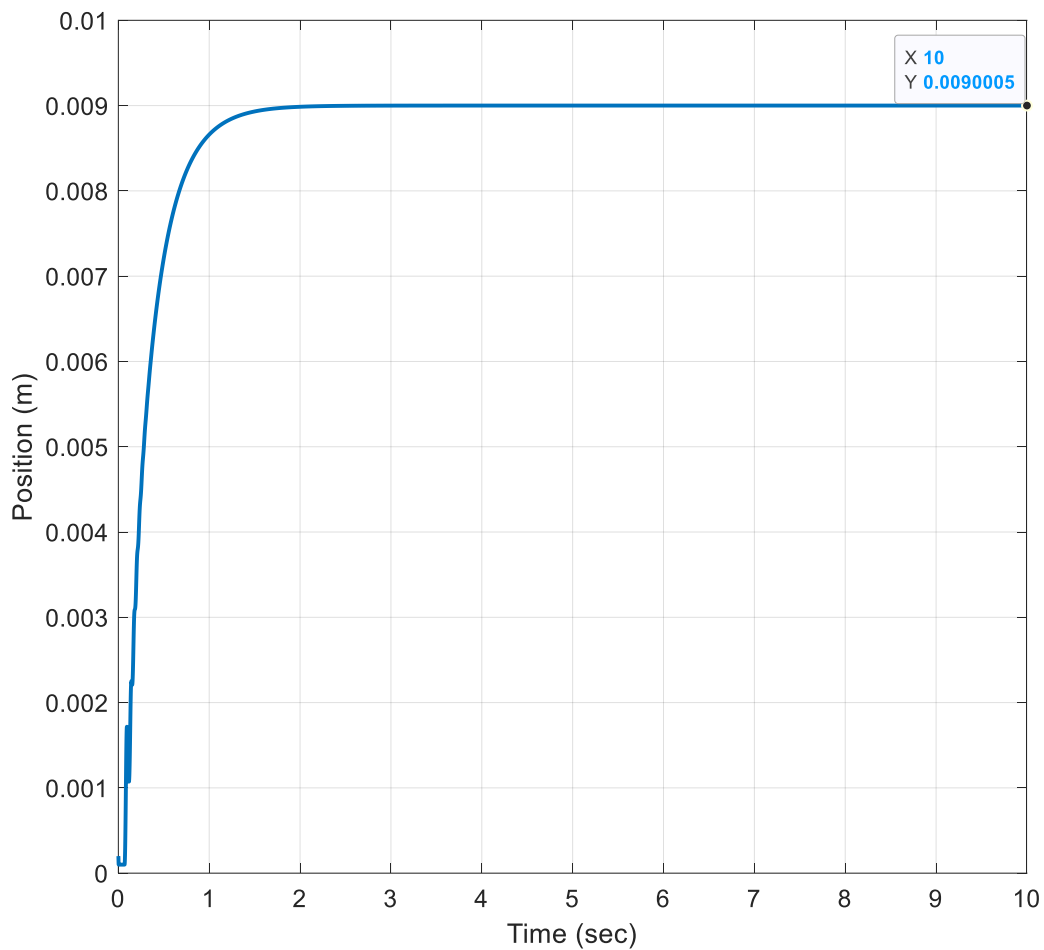
Figure 7. Position signal vs time starting at $2 \cdot 10^{-4}$ m

As shown in the above graph in Figure 7 the PD controller will give a relatively quick response time with smaller disturbance in the initial part. If the response time needed to be quicker as a result there can be seen overshooting in the position graph. After the ten second run time, the actual position can be seen as $9,0005 \cdot 10^{-3}$ m which means the system has a steady-state error of $5 \cdot 10^{-7}$ m. To be very thorough with the steady-state error, the simulation was run for a long time and this value was conclusively proved.
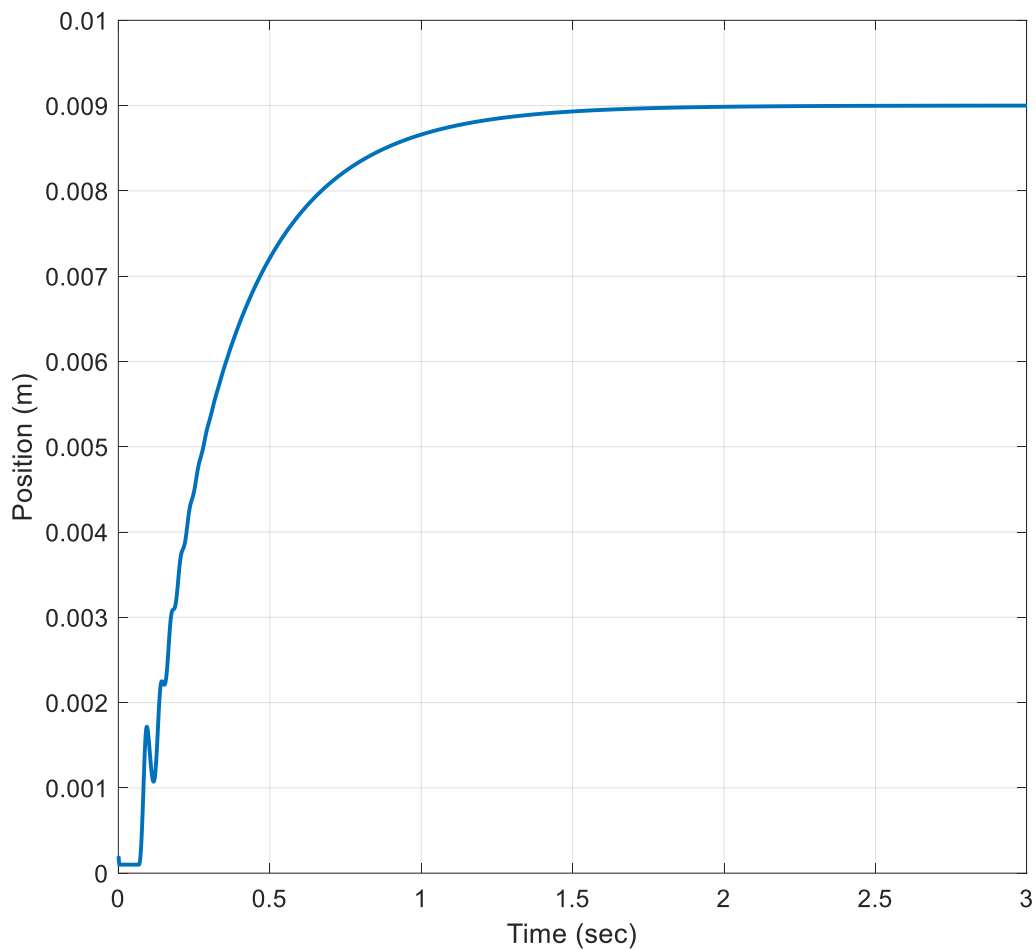
Figure 8. Position signal vs time for a 3-second runtime

Then the simulation is run for three seconds to get a clearer idea about the initial behaviour of the position parameter. As seen from Figure 8 the noise of the system is kept to a minimum. The initial fluctuation is due to the derivative part being relatively high by default. This can be avoided by reducing the derivative value but also will result in weaker control performance.
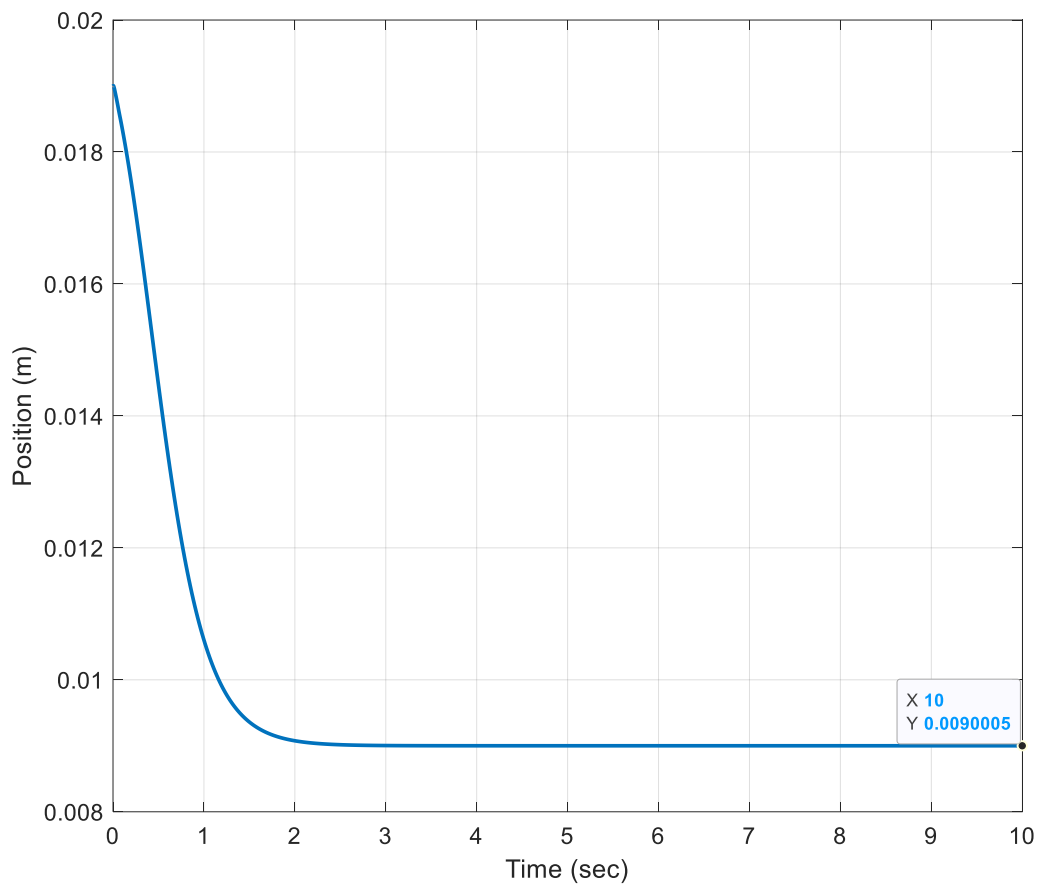
Figure 9. Position signal vs time starting at $1,9\cdot10^{-2}$ m

Next, the same simulation was run for 10s while the initial starting position is changed to $1,9\cdot10^{-2}$ m. Since the ball is moving upwards against the gravity the disturbance is comparatively low to the simulation which starts at $2\cdot10^{-4}$ m. In this simulation run as well after ten seconds of runtime, the steady-state error was seen at $5\cdot10^{-7}$ m. This can be seen on the graph in Figure 9 as shown.

To obtain the system behaviour without the PD controller the position error was given directly to the mathematical model and the simulation was run. The simulation setup without the PD controller can be seen in Figure 10 below.
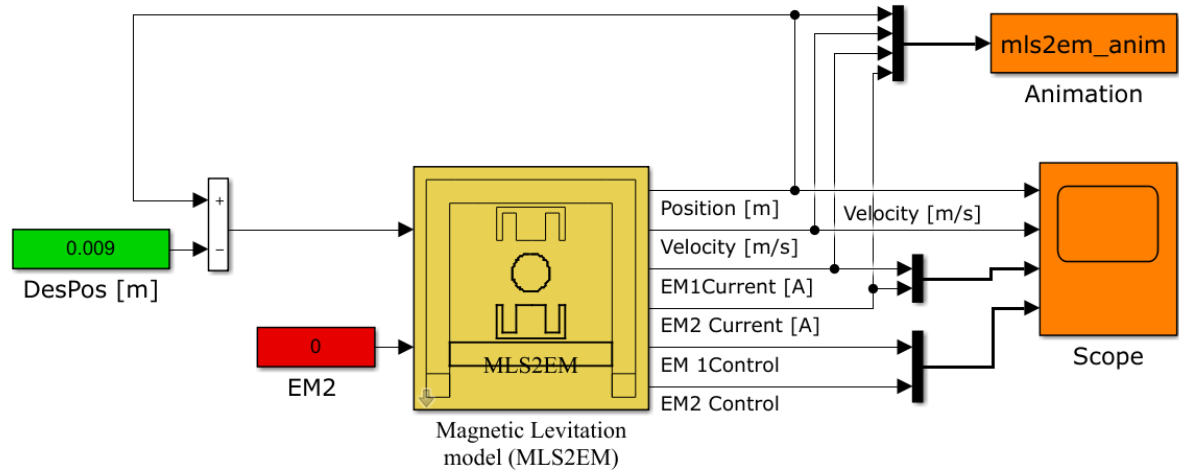
Figure 10. Closed-loop simulation model setup without the PD controller

From the initial state, the controller part was removed to observe the behavioural outcome of the metallic sphere. Since EM2 is zero it does not affect the outcome of the system. The initial starting point was kept at $2 \cdot 10^{-4}$ m to give the maximum travelling range when the sphere is free falling. In the free moving process, the position error will start from the negative range and will surpass the desired position and will travel to the positive position range giving an uncontrolled system. The visualization scope was connected to the Matlab workspace to plot position data graphically.
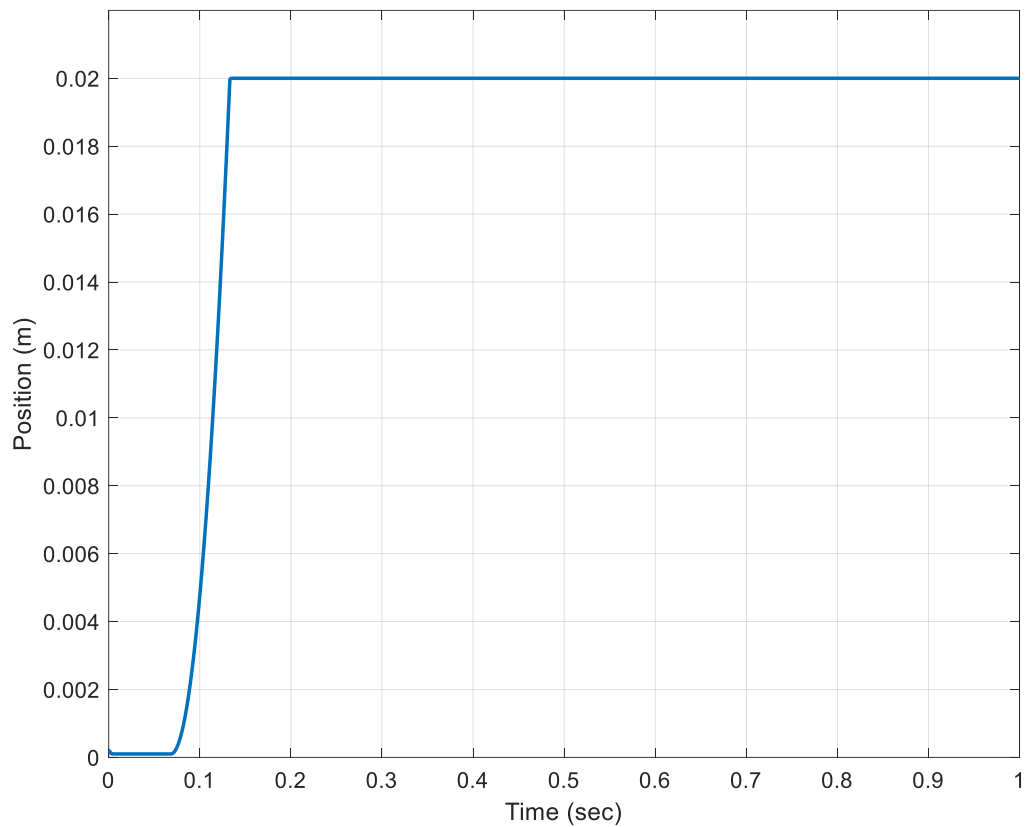
Figure 11. Position vs time without the PD controller

The simulation was run for three seconds and the graph was plotted as the Figure 11. Since the simulation was run freely without any controller and lower EM1 is also 0 the sphere is falling through the gravity. So in the simulation position graph and the actual system, $2 \cdot 10^{-2}$ m is the distance from the lower surface of the upper EM1 to the sphere's upper surface. But the upper saturation limit of the position parameter is also $2 \cdot 10^{-2}$ m so the graph will be clipped at that limit and stay in that value until the simulation stops. If the saturation limit was lifted off the position parameter will continue to increase with time.
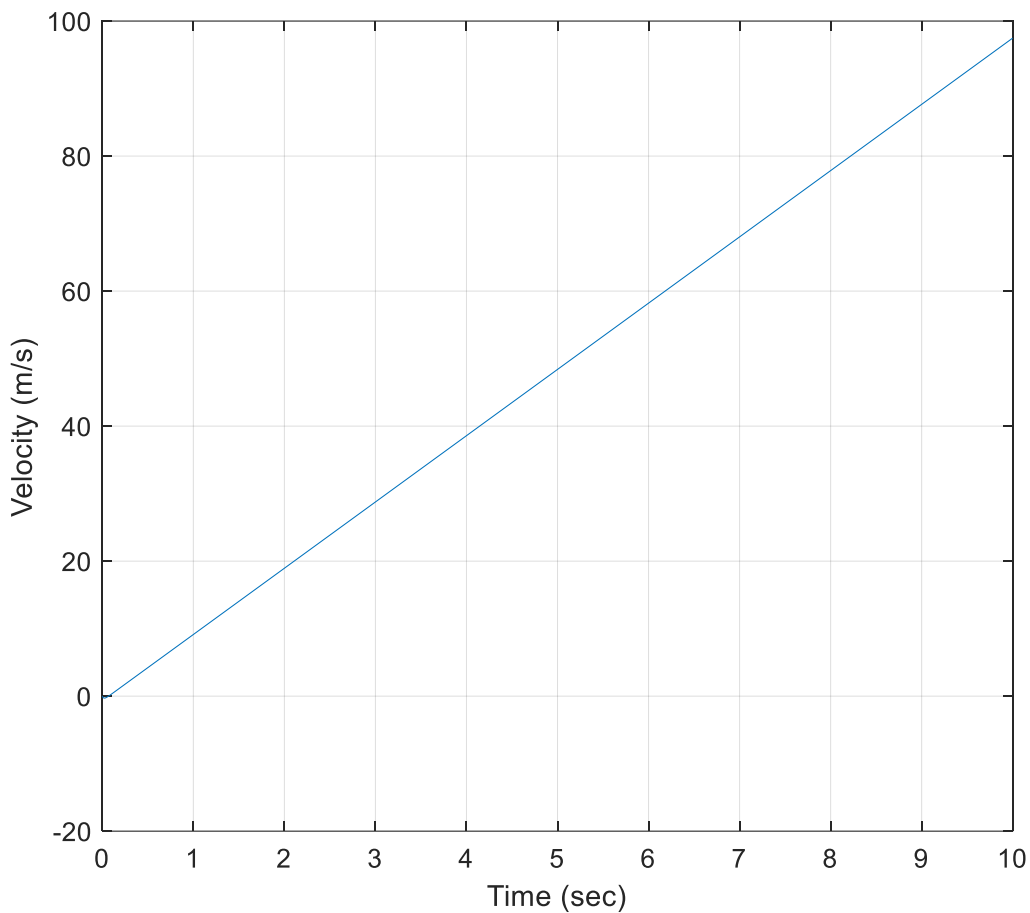
Figure 12. Velocity without PD controller for a ten-second runtime

Similar to position parameter velocity also increasing due to gravity with time giving an unbalanced control system. Since there is no saturation given to the velocity parameter it continues to increase with time. The graph in Figure 12, clearly shows that the sphere is free falling. From the increment of the graph gravitational constant can be obtained which is 9.81 m·s^{-2}.

3.3 Electromagnetic force vs Coil current comparison

For the control system to get the equilibrium at the desired position upper EM needs to have a specific amount of force generated from it to be able to balance the sphere at that certain point. To obtain the relevant force there needs to be a specific current running the coil of the upper EM. There needs to be a specific correlation between electromagnetic force, the coil current and the desired position. Clarify the connection between force vs desired position graph was taken as seen in Figure 13.
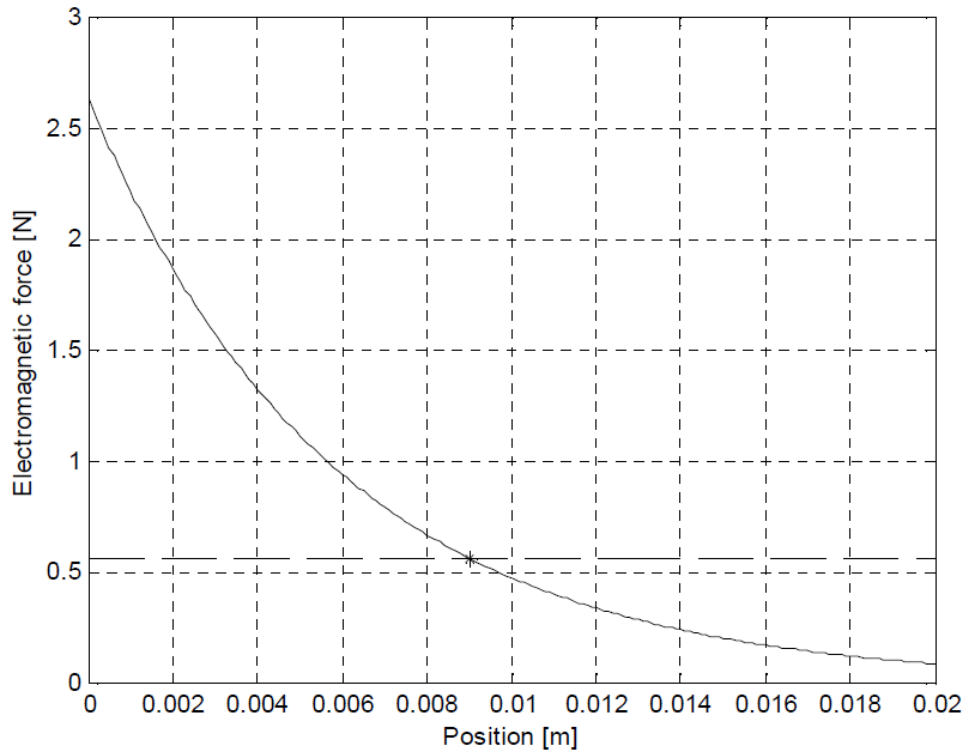
Figure 13. Electromagnetic force vs position for the metallic sphere [7]

The position distribution on the x-axis of the graph of Figure 13 ranges from 0 to upper saturation limit which is $2 \cdot 10^{-2}$ m. Resultant to that electromagnetic force distribution is plotted against the y-axis. When the position is zero is the point where the sphere is touching the upper magnet and has the highest force value. But to keep the sphere at the desired position of $9 \cdot 10^{-3}$ m the needed force will get from the y-axis interception to that point.

To get that amount of force needed to have a specific current running through the coil. To get the specific value a graph needed to be plotted between electromagnetic force vs coil current as in Figure 14.
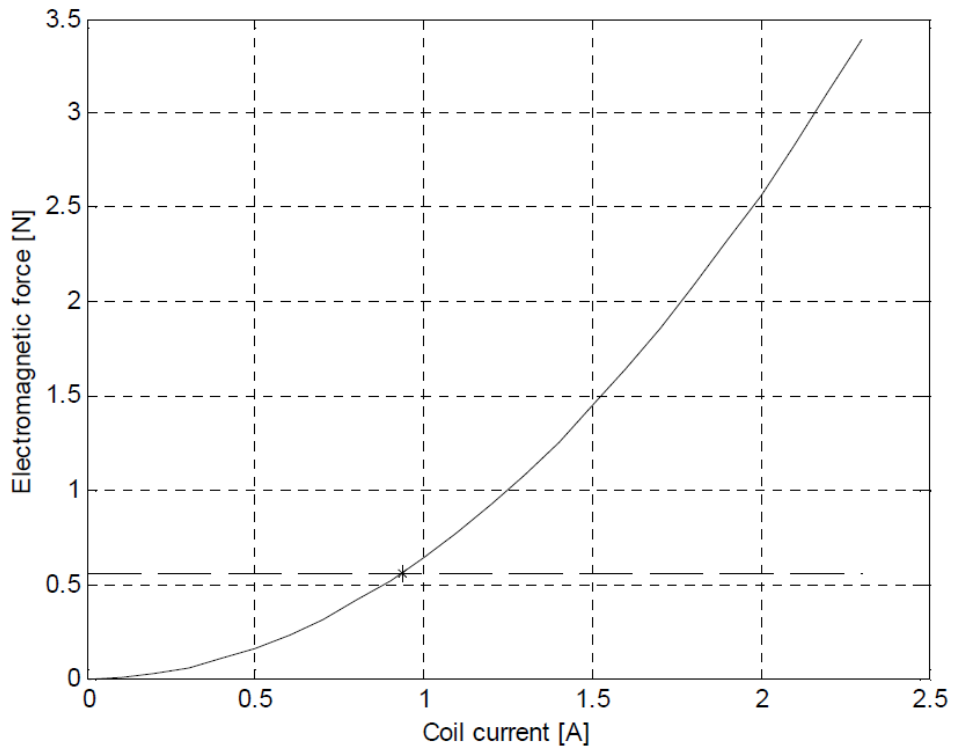
Figure 14. Electromagnetic force vs coil current [7]

Figure 14 was referred to as in coil current on the x-axis and the electromagnetic force is on the y-axis. From the electromagnetic value taken from Figure 13 by intercepting the point towards the x region, we can obtain the coil current needed to maintain the sphere in that position. The value obtains from the graph is 0,9345 A [7]. When replacing the controller the added new controller is needed to maintain this value to obtain the equilibrium of the sphere.

4. DEVELOPMENT OF THE FUZZY LOGIC CONTROLLER

4.1 Structuring and Initiating Plan

When designing and constructing a FLC there are four mandatory parts needed to consider which are fuzzification, fuzzy interface, fuzzy rule base and defuzzification [26]. The first part of to structure of the FLC is crisp inputs which are known as fuzzification and this can vary from a single input to multiple inputs depending on the situation [26]. During the fuzzification process, numerical input variables are converted to membership functions. The next part is known as the fuzzy interface which will be accumulating the membership function and with given rules will create a logical output (AND or OR) of fuzzy sets. Finally from these fuzzy sets through defuzzification, a quantifiable output will be taken.

This process can be represented in a much simpler way therefore the structure of the FLC can be illustrated using a block diagram as shown in Figure 15 below,
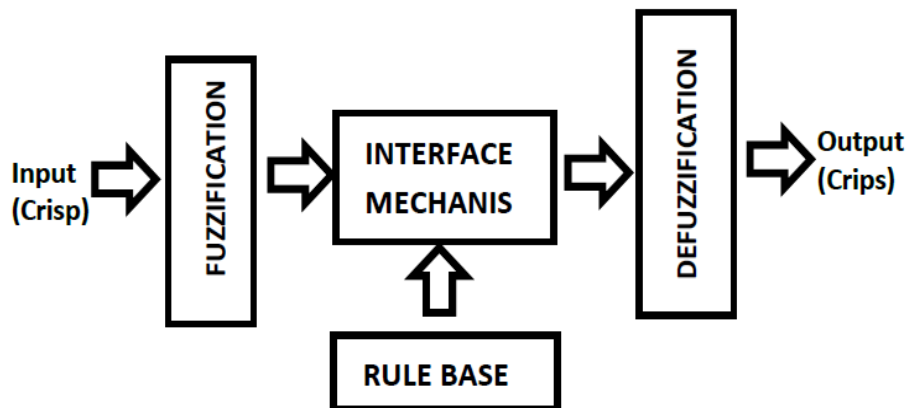
Figure 15. Block diagram for the FLC [26]

Before structuring begins there needs to be a rough analysis regarding how many input functions and how many outputs function needed to consider. This consideration purely depends on the experiment structure. For replacing the PD controller in MLS2EM which needs two inputs for proportional, derivative variables and one output for control. If the replacing controller is PID then additional input should be generated extra for an integral part of the system.

4.2 Data Acquiring for Parameter Ranges

Since the FLC will be replacing the PD controller, two inputs needed to be considered are error as in the proportional variable input and change of error as in the derivative variable input. To acquire the needed data the error and change of error inputs were connected to a MUX and directly given as input for the mathematical model.

The simulation model without the controller can be seen in Figure 16 below.
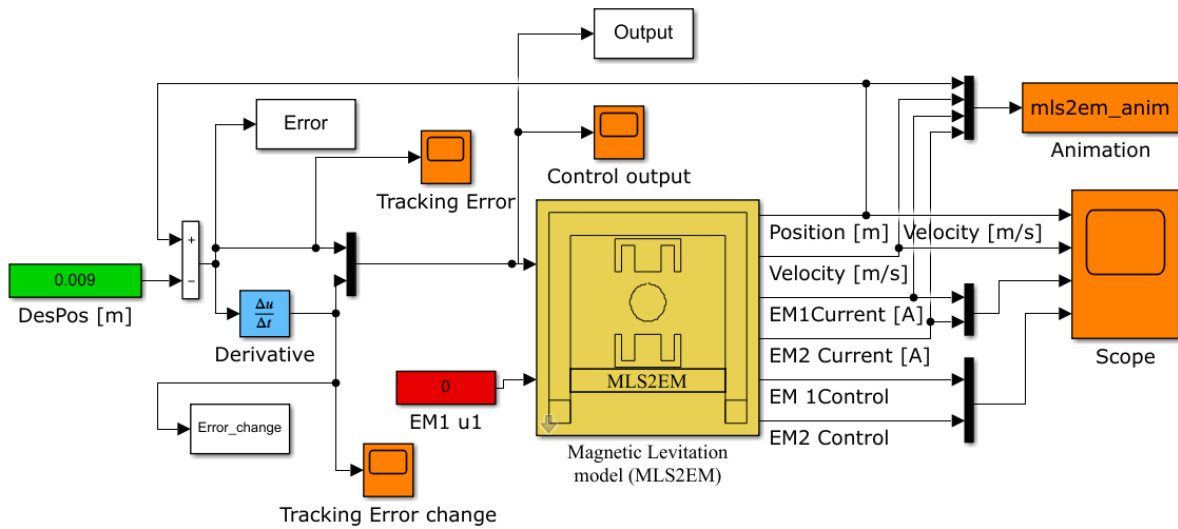
Figure 16. Simulation model without the FLC

The Simulink control system was modified by additional three scopes to the visualization section (orange) to observe the I/O behaviour of the system. The position error was split into two channels and an additional derivative part (blue) was added to obtain the change of error. All three parameters were given function blocks that can be connected to the Matlab workspace.

Thereafter the simulation was run for the closed-loop system without any controller. Both input data for Error, Change in Error and controlled output data were saved into Matlab workspace for future use while designing the Fuzzy logic controller. After the simulation run workspace data (Error, Error_ Change, Output) were referred to get the maximum and minimum ranges of inputs and outputs for FLC design.

4.3 Fuzzy Logic Controller Design

Firstly before the designing process begins user must install the "Fuzzy Logic Toolbox" for the Matlab environment. Next type "fuzzy" in the command window and the Fuzzy logic design window will appear as in Figure 17.
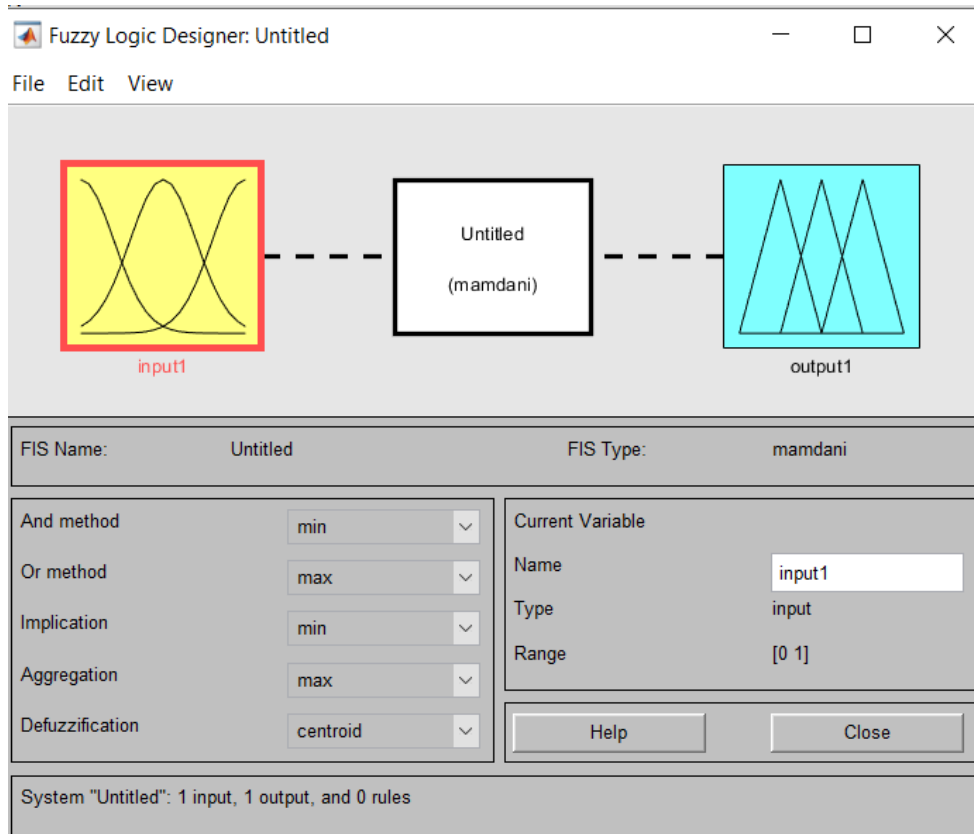
Figure 17. Fuzzy Logic Designer interface

The interface mainly consists of three parts input, output, and Mamdani system. Mamdani system contains all the logical rules and logical conditions when applying conditions using rules. Additional variables can be added for both I/O from the edit tab depending on the control requirement.

Since the control system for MLS requires two inputs and one output the flow spread for the controller design interface can be shown as in Figure 18. The acquired data range was given to each I/O variable.
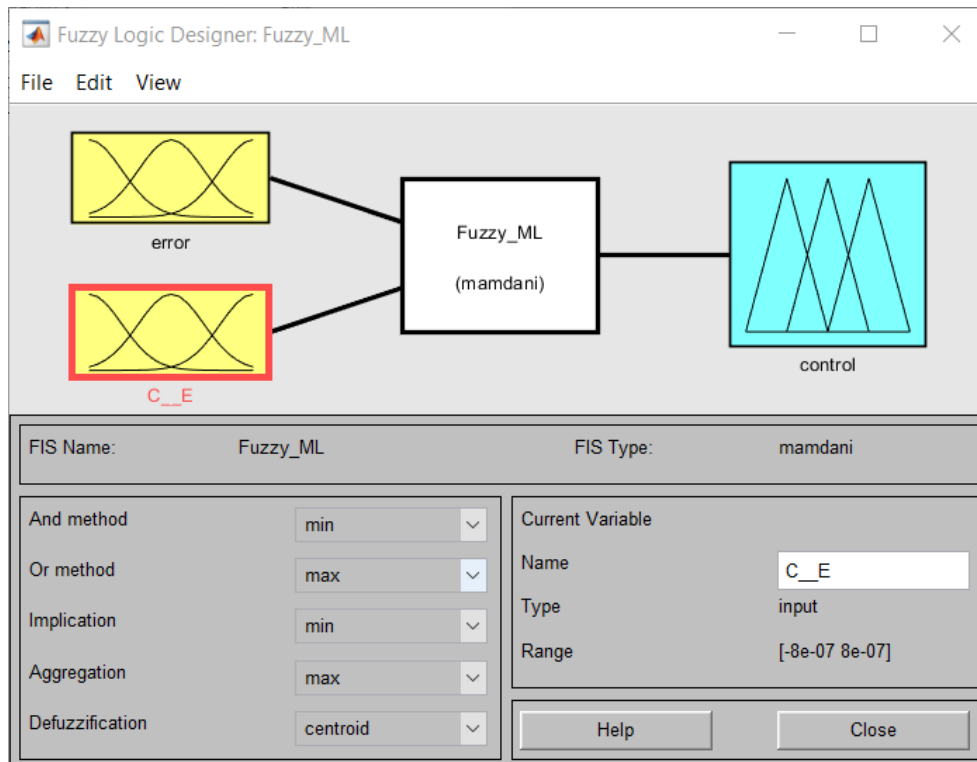
Figure 18. Fuzzy Logic Designer interface for the control system MLS2EM

4.3.1 Range selection for membership functions

During the FLC design process membership functions for each input needs to be determined. According to the number of membership functions for each input, the result for the number of total rules and conditions are taken for the control system. Initially, three membership functions were taken each for input variables. Later in the experiment, the membership functions were increased by five for each input for a much smoother distribution for the control output. Except for the two far ends of the spectrum membership functions, all the rest of the functions were used as in triangular function type to get more uniform output results. Mostly for the Mamdani interference system the triangular membership functions are used. Essential to ensure the mapping between the membership functions so that they would be overlapping from one region to another to give a continuous and robust result for the control system. All the I/O parameters should have a symmetrical spread over the value 0. Hence it will have an equal and opposite distribution on either side of this median value of 0.
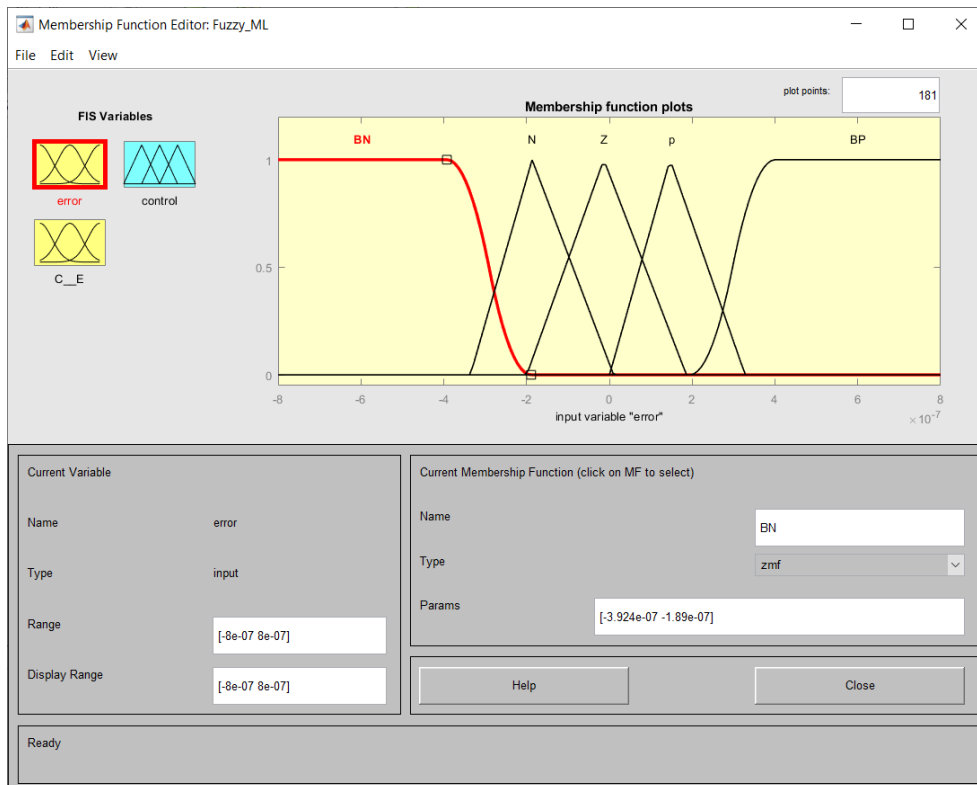
Figure 19. Error input membership function plots

From the acquired data both error and change of error should have similar membership pattern plots to have a robust control system. For that, both error and change of error should be closing on the value 0. The logical outcome of the control system will be discussed later in the chapter. As seen in Figure 19 for the far end of the membership functions BN and BP have used the zmf function type so when the offset is high from the setpoint it will change the error rapidly towards the triangular function making the whole control system quick responsive and efficient.

When the error function is in the triangular region depending on the change of error value the controller will push the error value through the intercepted triangular region until the value is 0. Even though the error is zero it is not enough for the control system to be stable at the given desired position of $9 \cdot 10^{-3}$ m. At this error value of 0, the change of error can be either negative or positive depending on that FLC should adjust its control value accordingly.

Figure 20. Change in Error input membership function plots

Considering the change of error function plots the total range was set as the same as the error function but the membership function plots were adjusted as Figure 20 according to control behaviour. Depending on the error value being negative or positive and change of error being negative or positive the sphere can both reach the setpoint from either end or can be going away to either side.

Assume the change of error is 0 at a given moment and if the error is also zero at that given moment then the sphere is at its desired position of $9 \cdot 10^{-3}$ m. But if the error is positive or negative it will remain positive or negative since the change of error is 0. Hence the controller needs to change the output resulting in both error and change of error should reach value 0. Both input ranges were taken from $-8 \cdot 10^{-7}$ to $8 \cdot 10^{-7}$ since the acquired data is within the range limit.
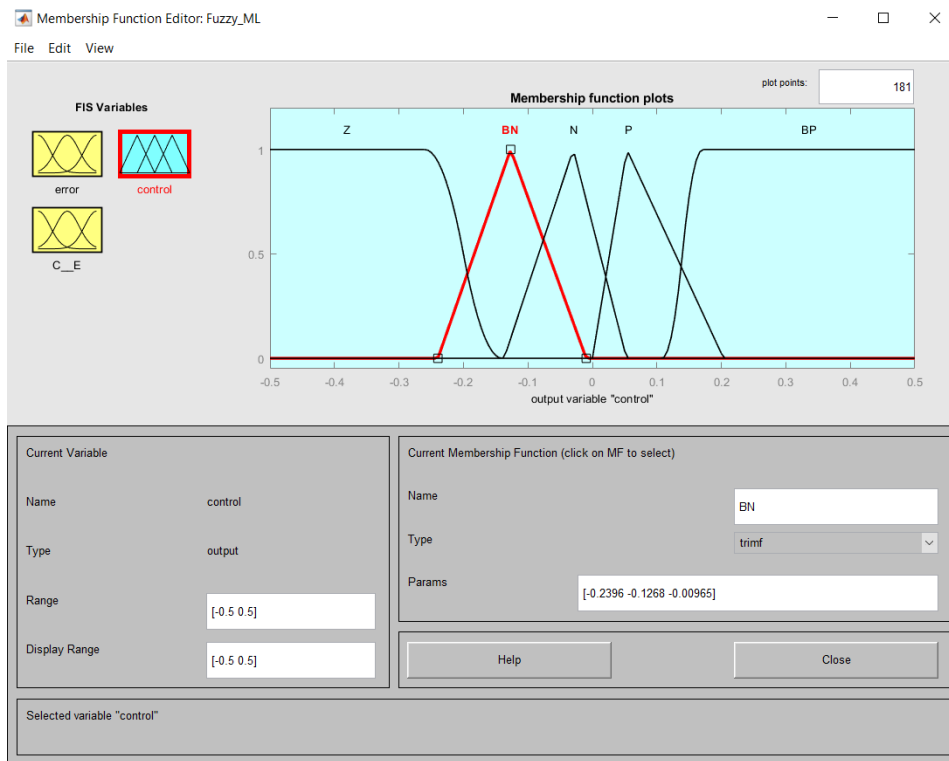
Figure 21. Control output membership function plots

Finally, the control range was set to -0,5 to 0,5 as in Figure 21 hence the acquired data is within that range. The parameter ranges were set according to error and change of error. For the control signal as well it's essential to have overlapping membership functions so the controller will move through the ranges uniformly and continuously.

4.3.2 Rule selection matrix

The next edition of the design process is assigning the rules for the FLC. The number of rules can be decided according to the equations below.

$$Number\ of\ rules = A \cdot B \qquad (4.1)$$

$$Number\ of\ rules = 5 \cdot 5 \qquad (4.2)$$

$$Number\ of\ rules = 25 \qquad (4.3)$$

Where

A - Number of membership functions of the first input
B - Number of membership functions of the second input

These rules should be defined in matrix form as in Figure 22 which the first input of each membership function must be arranged in the first column of the rule table and the second input must be inserted in the first row of the rule table.

e	ez-1	BN	N	Z	P	BP
BN		BN	Z	BN	Z	Z
N		Z	N	N	Z	Z
Z		BN	N	Z	P	BP
P		Z	Z	P	P	Z
BP		Z	Z	BP	Z	BP

Figure 22. Rule selection matrix for the FLC

In the given rule Figure 22 each component is denoted as below,

BN - Big negative
N - Negative
Z - Zero
P - Positive
BP - Big positive
e - Error
ez-1 - Change of error

The inputs are highlighted in the grey area in Figure 22 and the resultant control outcomes are denoted in the white area which concludes a 5·5 matrix. The assigned rules always start from the first row and first column of the matrix (white area) and go right side and downwards. The control system which behaves the same around the setpoint has similar rules through the diagonal access of the matrix. When selecting the first rule it should be if the error is Big negative and change of error is also Big negative then the output will be Big negative. From there, onwards rules can be selected row-wise or column-wise and the outcome result of the rules will be the same. But to function the rules in the FLC these needed to add through the rule editor with a logical operator. Since error and change of error both need to obey the conditions those inputs are essential to be connected by logical AND operation in the rule editor. Then the twenty-five rules were added using logical AND operation as in Table 4.1.

Table 4.1 Designated rules for the Fuzzy Logic Controller

No	Error	Logical operation	Change of error	Control
1	BN	AND	BN	BN
2	N	AND	BN	Z
3	Z	AND	BN	BN
4	P	AND	BN	Z
5	BP	AND	BN	Z
6	BN	AND	N	Z
7	N	AND	N	N
8	Z	AND	N	N
9	P	AND	N	Z
10	BP	AND	N	Z
11	BN	AND	Z	BN
12	N	AND	Z	N
13	Z	AND	Z	Z
14	P	AND	Z	P
15	BP	AND	Z	BP
16	BN	AND	P	Z
17	N	AND	P	Z
18	Z	AND	P	P
19	P	AND	P	P
20	BP	AND	P	Z
21	BN	AND	BP	Z
22	N	AND	BP	Z
23	Z	AND	BP	BP
24	P	AND	BP	Z
25	BP	AND	BP	BP

The Rule Editor after adding the rules can be seen in Table 4.1 and since the rules were added column-wise change of error seems to be the same from rules one to five and according to the error value the control region was selected. After every five rules, the change of error range is changing giving all the twenty-five rules essential to control the system. To get an even more comprehensible idea regarding the range shifting, the rule viewer can be used in the design interface which is shown in Figure 23.
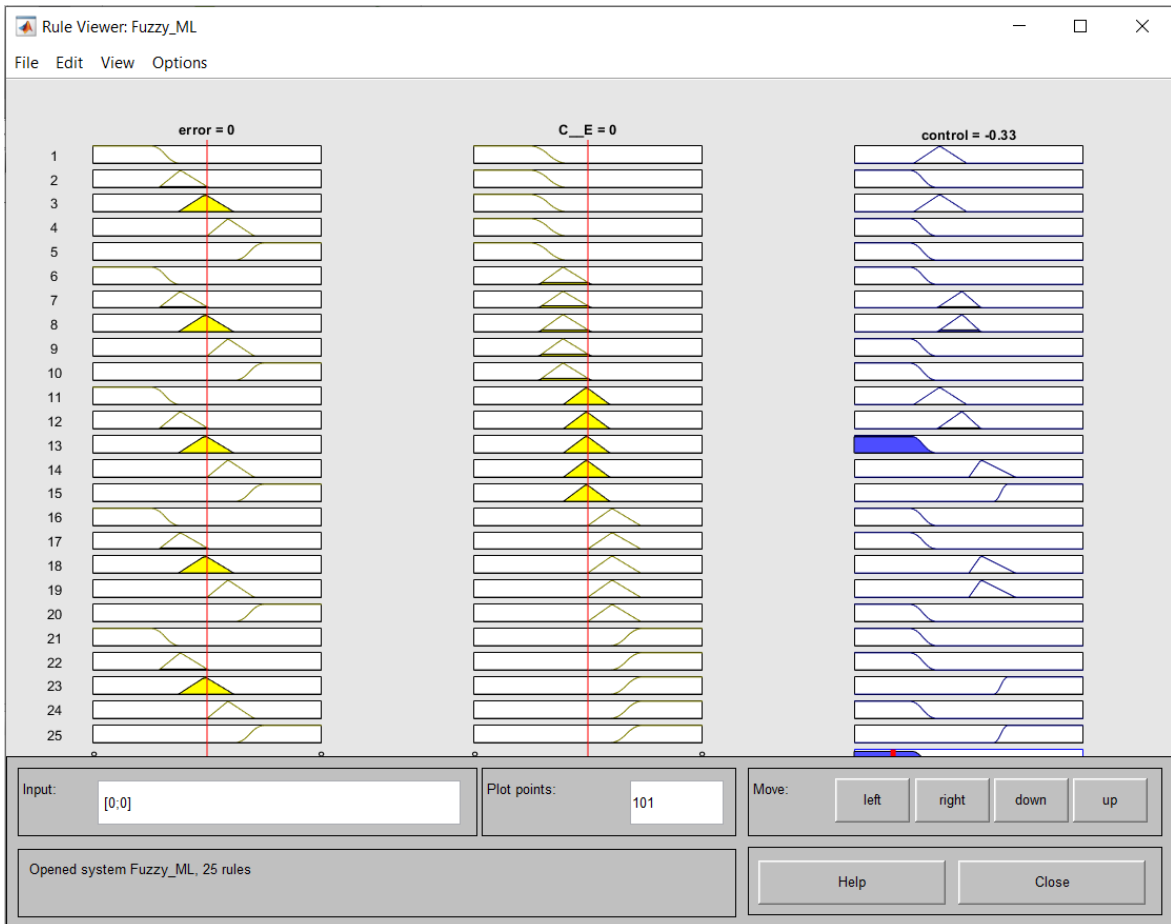
Figure 23. The Fuzzy rule viewer interface

The Fuzzy rule interface is used to monitor the range shift of output due to variable changes in inputs. For the instance shown in Figure 23, the error and change of error are zero and the colour yellow states the number of rules which will be in that region. Rule number 13 shows it is dominant in both variables and hence the output will be in the Z region as shown. As the membership function regions of error and change of error continue to change, the control output will change its cause to relevant regions as shown in the rules. Because all the membership functions are overlapping any region would not have a hundred per cent occupancy and all the region are built to shift from one to another due to changes. This can be seen in Figure 23 where the change of error has the dominant region from rules 11 to 15 but also has a small amount of occupancy from rules 6 to 10. The same behaviour can be seen on both the error input and the control output. After designing the FLC it needed to be added to the workspace after saving it as a FIS file.

4.3.3 Overview of the parameters

The parameter ranges we considered and explained for I/O could be graphically plotted one variable against another. To obtain the control value against each input, the relevant input should be selected to the x-axis and the y-axis should be set to none so the graph will plot as x vs z (output).
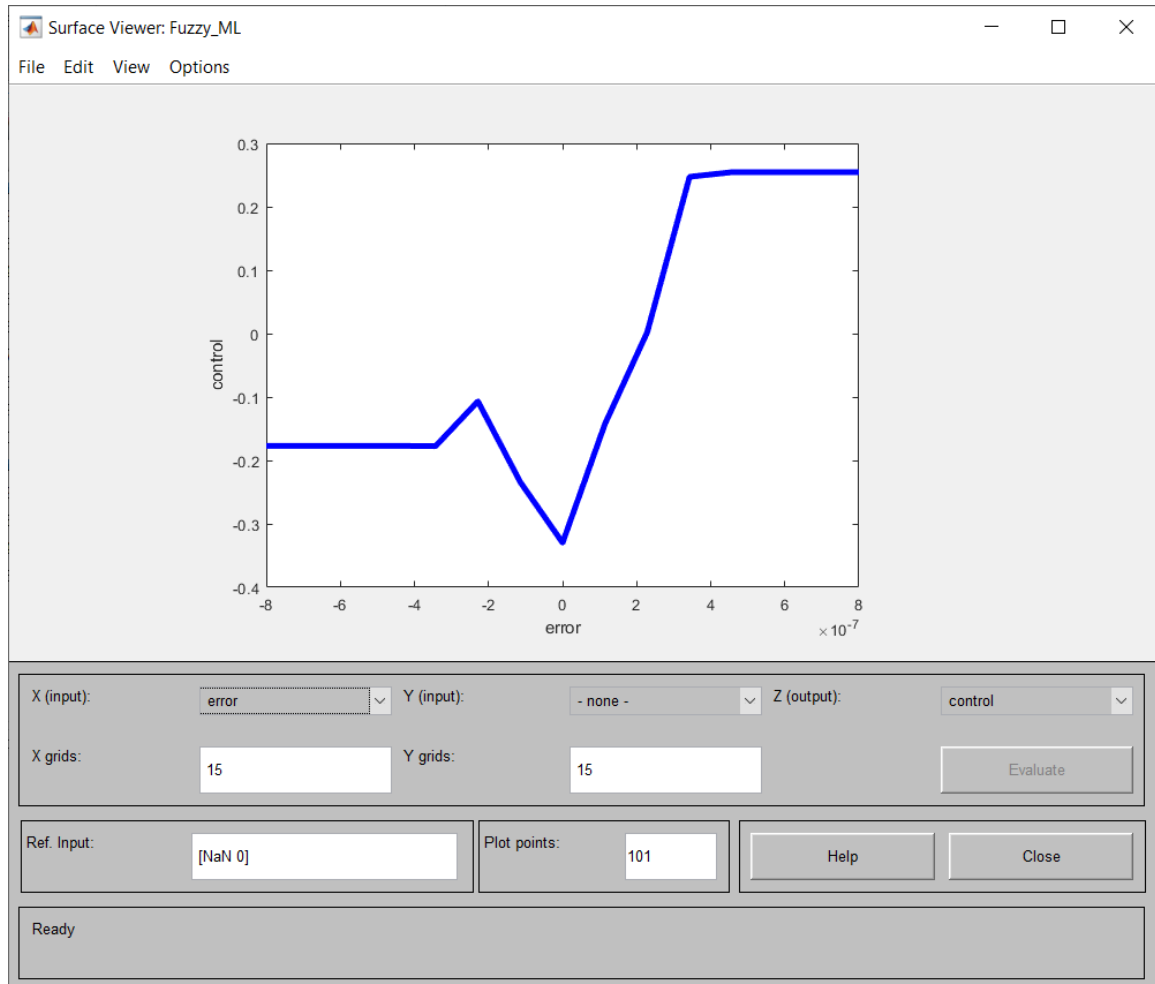
Figure 24. Error vs control membership distribution

In Figure 24 the behaviour of the control function can be seen due to the error function changing through the range. When the error value is zero the control value has its minimum value. From zero value onwards in the positive direction in the x-axis, the control parameter has a positive increment. The maximum control value is obtained when the error is maximum in the given range which is $8 \cdot 10^{-7}$ m.
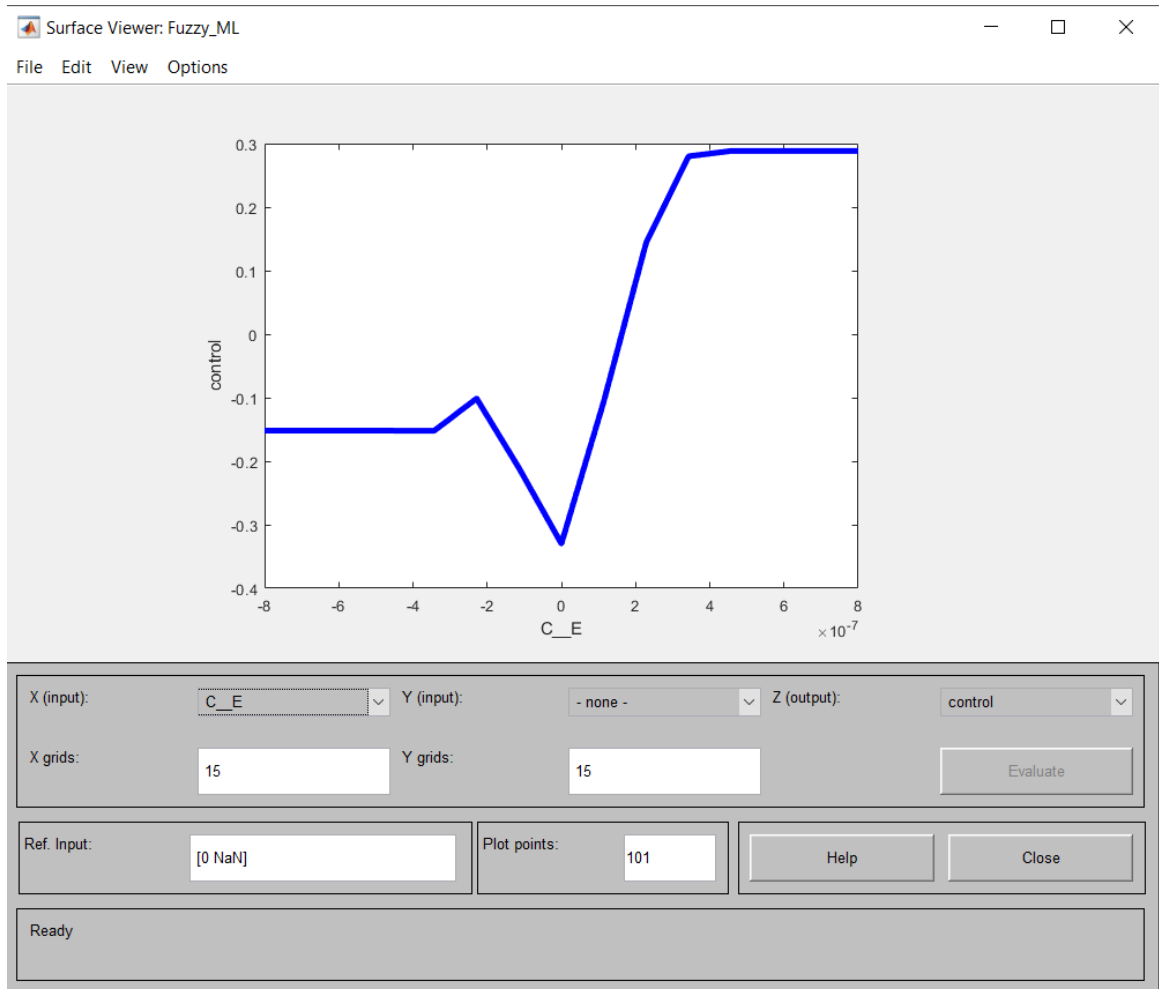
Figure 25. Change of error vs control membership distribution

Next, considering the behaviour of the membership plots between the change of error and control can be seen in Figure 25 as above. Since the membership plots for change in error are almost the same compared to error membership plots the outcome of the control graph is similar as well. When the change of error is zero the control value is the same as the control value when the error is zero.

The parameter view can be changed and all the three variables can be plotted in 3-dimensional space as shown in Figure 26. This allows getting a better overview of how the parameters are aligned from region to region.
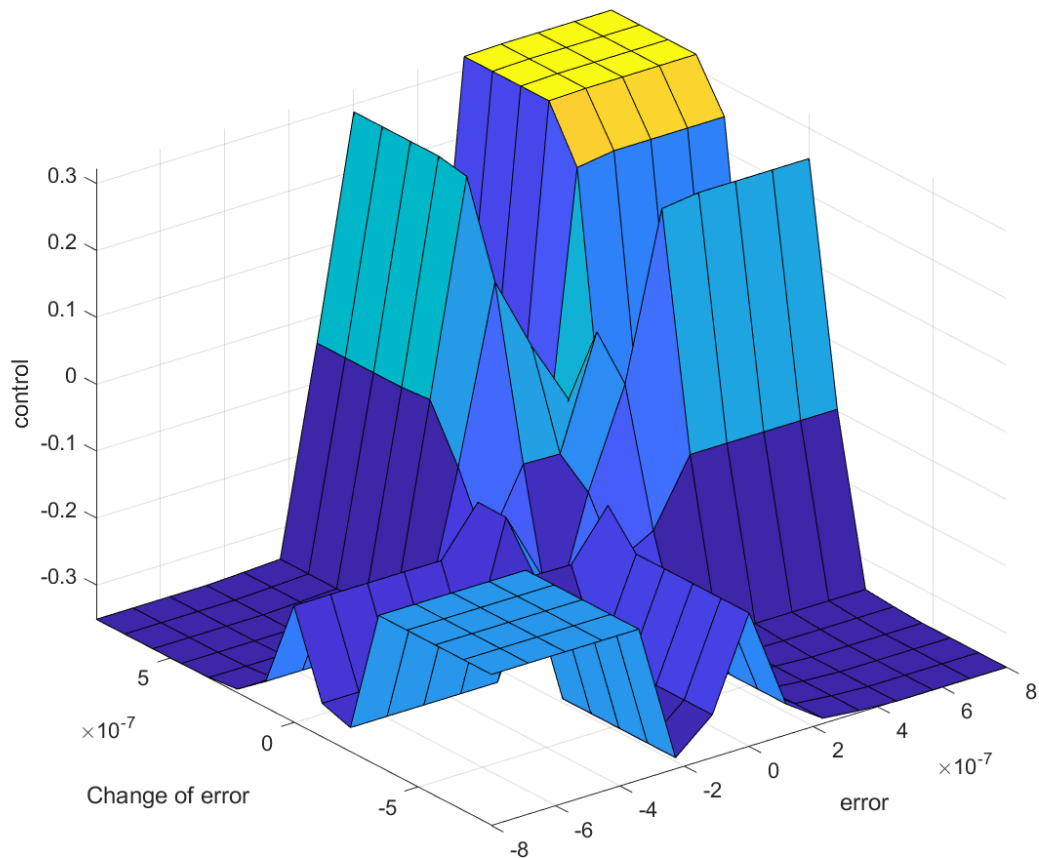
Figure 26. 3-Dimensional view of the I/O membership plots

Both x and y-axis have the same range due to error and change of error being same range and the control was denoted in the z-axis. When the error and the change of error are maximum control region can be seen on the yellow region which is maximum at that point. As discussed in earlier chapters control require to have a higher output to bring the sphere towards the setpoint. Other regions abide by the same theory as the 25 rules which was initially given. Similar to the matrix behaviour the 3- dimensional view is also having an almost symmetrical distribution.

4.4 FLC Simulation Run

Before the final simulation is run the saved ''Fuzzy_ML.fis'' file was added to the Matlab workspace and the PD controller was replaced with FLC. The fis file was loaded to the FLC and the simulation was run. The final replaced Simulink setup can be shown as in Figure 27.
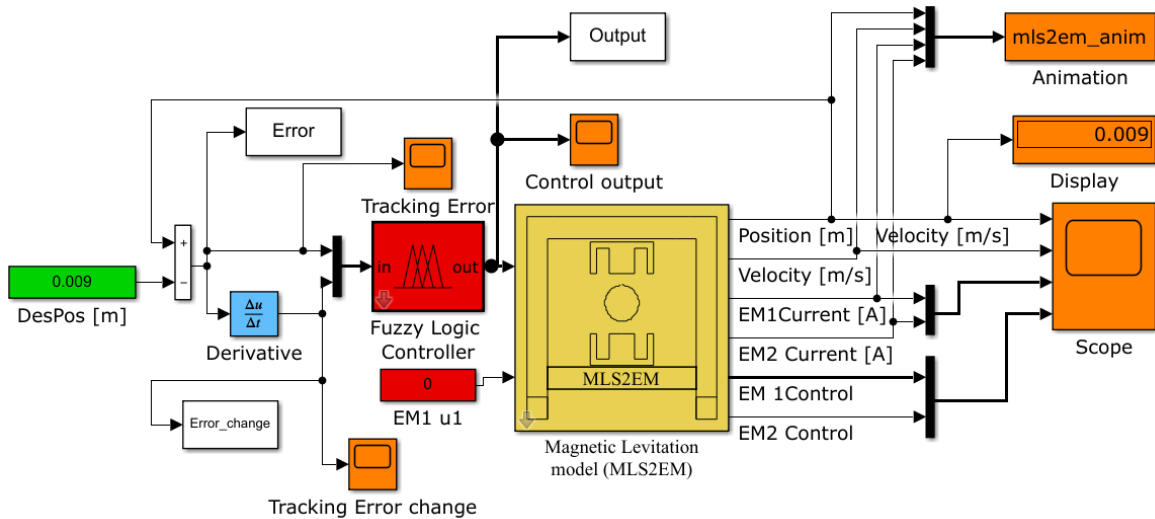
Figure 27. Completed Simulink setup after FLC replacement

Both error and change of error were connected through mux and connected to FLC as in Figure 27. Unlike the PD controller, the mux will carry two signals inside FLC (red) rather than one. After the simulation has begun under two seconds the position of the sphere reaches the desired value of $9 \cdot 10^{-3}$ m as shown in the display of Figure 27. All the I/O's for the FLC were given to separate scopes to observe the behaviour of each variable graphically.

Both Error and Change of error was monitored in the desired position to observe the offset and come to an understanding regarding the stability of the system. When starting from the desired position after one second run time error can be plotted as in Figure 28. The intention behind running a smaller time frame is because most of the sensitive movement starts at the beginning of the simulation and after the controller reaches its steady-state level no fluctuations can be seen. Since the FLC is a quick response needed to take an early small time frame to observe the behaviour.
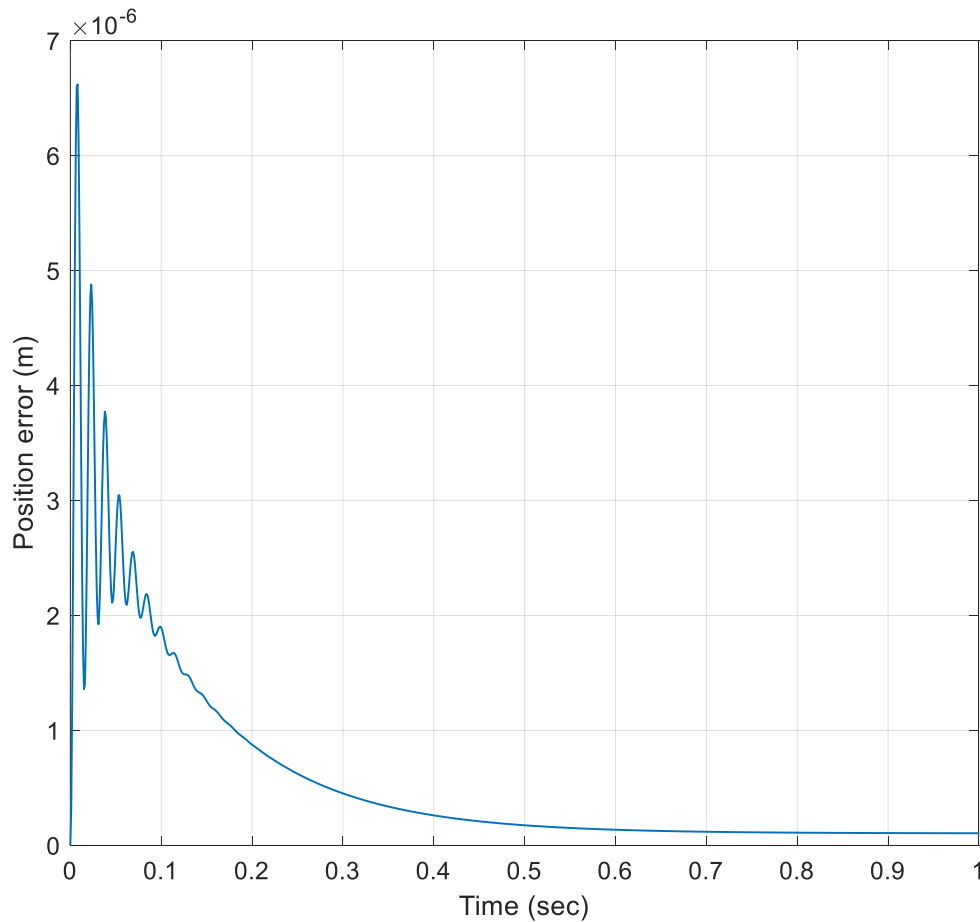
Figure 28. Position error vs time when the sphere is at the desired position

When the start of the simulation error has a small positive value since due to gravity ball is travelling downwards and the value of the actual position will be marginally higher than the desired position of $9\cdot10^{-3}$ m. According to the rules, the error is shifting from a big positive range into the positive range and finally into the zero range. After the one second limit, the error is keeping a very low and constant value almost close to zero. The reason is due to the very minor difference between zero and the actual value is caused by steady-state error.

At the same starting moment change of error was also monitored for a one-second time range as shown in Figure 29. At the starting point, the desired position is the same as the actual position and the initial velocity is zero so the change of error should start as zero.
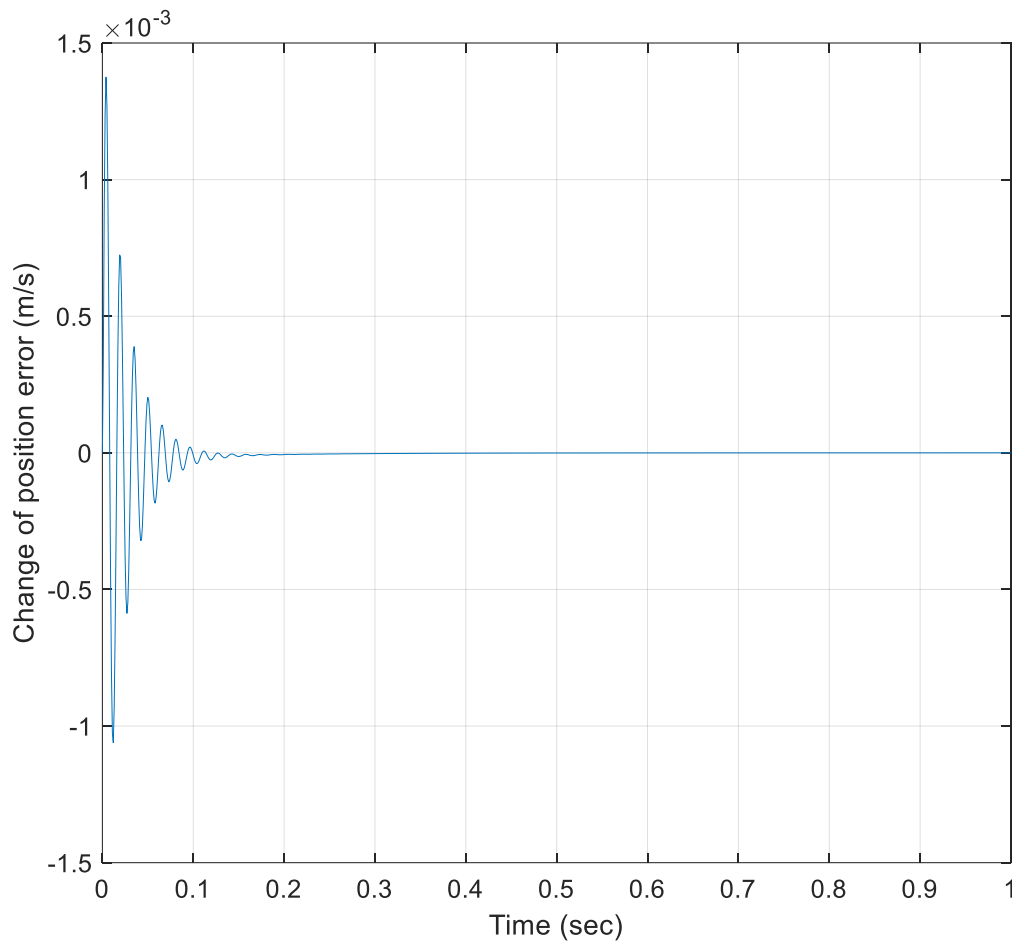
Figure 29. Change of error vs time when the sphere is at the desired position

Same as the error parameter, when the start of the simulation the sphere is reluctant to stay in place due to gravity and the fuzzy controller will pull it back towards the setpoint of zero. This creates a small simple harmonic motion with a small amplitude around setpoint zero. Unlike error parameter change of error reaches the zero limit both in simulation and in the actual system.

4.5 FLC real-time system

After the simulation was done the FLC was connected to the real system that will be replacing the mathematical model with the actual model. FLC which has two inputs, a derivative part and a mux was inserted into a subsystem to make it visually aesthetic. The FLC which was connected to the actual system can be seen in Figure 30.
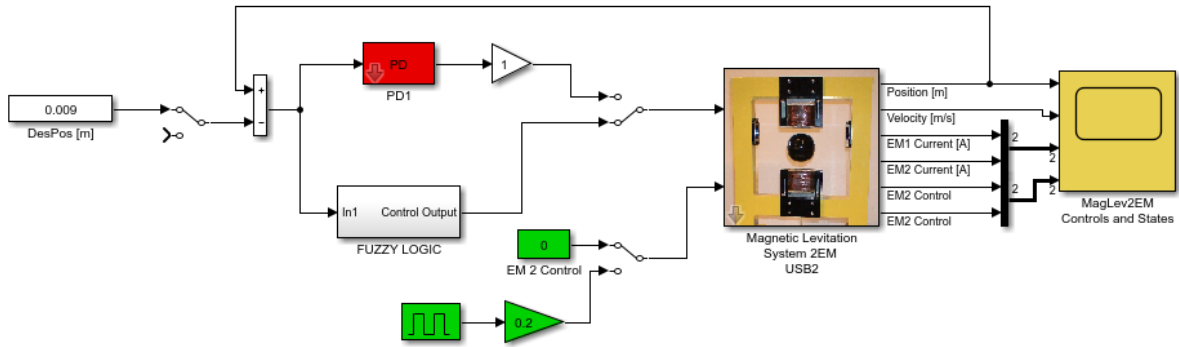
Figure 30. Control system with FLC connected to the actual model

For an additional expansion to the thesis, a small pulse disturbance was added to the lower magnet through a manual switch. The system was run for both occasions where the EM2 value is zero and for the pulse disturbance. The pulse was kept at 0,2 amplitude to keep the sphere within the operation range. The system operating in real-time with the FLC can be seen in Figure 31.

Figure 31. Control system with FLC connected to the actual model

In the actual model as seen in Figure 31, the metallic sphere is balancing at the desired position of $9 \cdot 10^{-3}$ m. The FLC is monitoring the actual position by the position sensors located on either side of the frame to calculate how much light passes through the gap between upper EM1 and the metallic sphere. This thin light film represents and determines the distance from the lower surface of the upper EM1 and the metallic sphere.

5. RESULTS

This Chapter is primarily focused on the comparative analysis between the outputs of PD controller and FLC. The data acquisition and data range selection for the results were discussed in previous chapters. The chapter also discusses the results for different time ranges because control systems behave completely inconsistent in different ranges. Some instances will require quick reaction times and responses to maintain the smoothness and accuracy of the whole control system. When plotting and comparing graphs from PD controller and FLC depending on their viewing range some parameters are viewed together and plotted to get a much more accurate comparison between the two controller types. Some parameters such as control PWM are observed separately to get crucial data without and overlapping.

To cross relate the behaviour of each parameter the Simulink system was kept unchanged for each instance apart from the controller change. The data for each controller was added to the Matlab workspace in separate matrices and plotted in the time domain. The results were taken from both ends of the spectrum close to the upper and lower saturation end of the position parameter. The main persuasion regarding taking close to the end limits of saturation is this being the highest probability to happen to overshoot or undershoot of the control system.

The most pre-eminent one of all the parameters is the position parameter. Because reason being the whole objective of the experiment was to achieve the sphere's desired position of $9 \cdot 10^{-3}$ m. Both controllers were able to achieve this. To compare which controller performed better, both of the results were plotted in the same graph as Figure 32 for five seconds run time starting the simulation from $2 \cdot 10^{-4}$ m initial position.
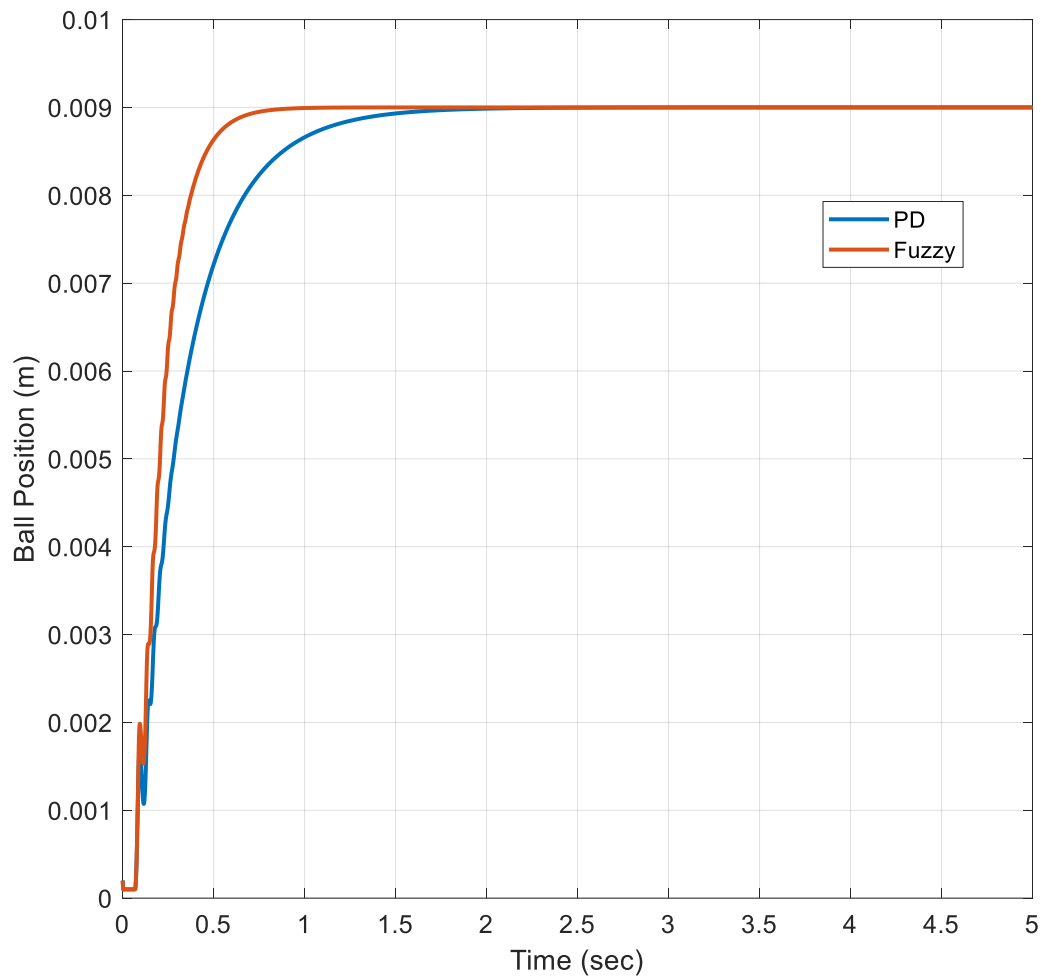
Figure 32. Position parameter for PD vs Fuzzy starting from $2 \cdot 10^{-4}$ m

The plotted graph in Figure 32 show comparatively fuzzy logic controller is much quicker responsive compared to the PD controller. And the main purpose being FLC is switching between the regions much quicker while PD is changing the derivative component as time flows. FLC was able to achieve such a quick response time without any overshooting or undershooting. The PD was tuned by default for its optimum level and if it was much quicker overshooting and undershooting can be seen. This is why FLC is optimum for non-linear systems compared to PD.

To compare the steady-state error behaviour of the two plots need to take a closer and extended view at the five-second mark since the error value is very minimal. The enlarged view for the steady-state error can be seen in Figure 33.
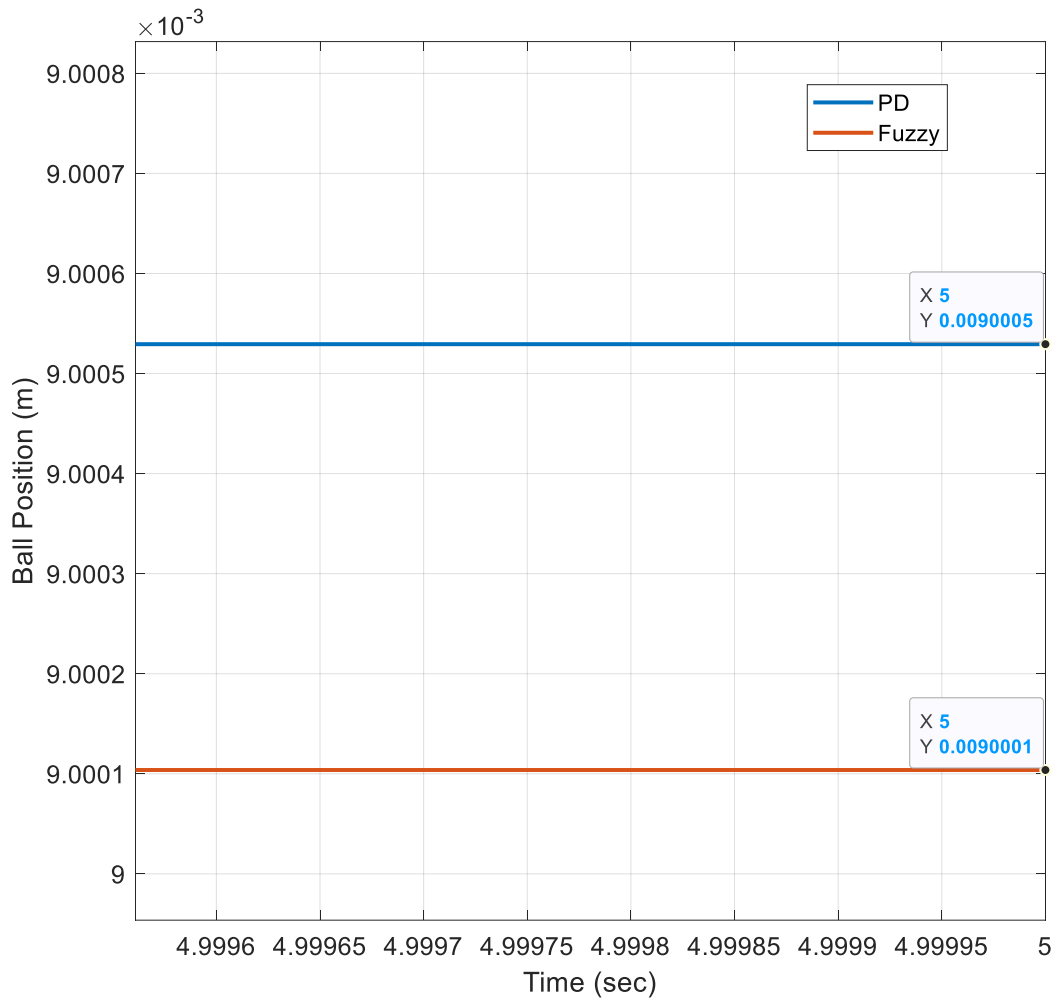
Figure 33. Steady-state error for PD vs Fuzzy starting from $2 \cdot 10^{-4}$ m

The enlarged view of the position graph in Figure 33 denotes FLC has a low steady-state error of $1 \cdot 10^{-7}$ m compared to the steady-state error of PD which is $5 \cdot 10^{-7}$ m. Steady-state error is much more accurate when the furthest point was considered. The values were proven by lengthening the simulation time.

Similarly, the initial starting position was changed to $1,9 \cdot 10^{-2}$ m and the simulation was run for five seconds and both FLC and PD results were plotted in the same graph as in Figure 34.
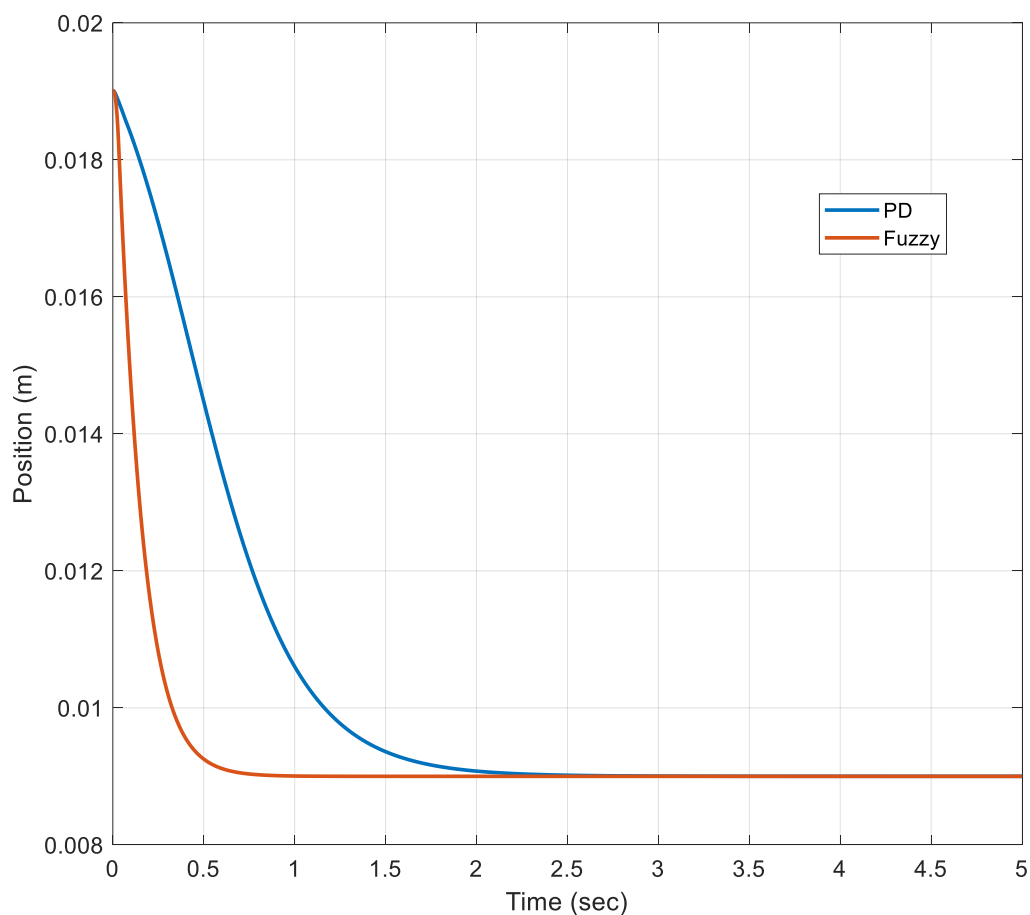
Figure 34. Position parameter for PD vs Fuzzy starting from $1{,}9\cdot10^{-2}$ m

Even considering the starting point close to the upper saturation limit the results are similar to the lower saturation plot, in which FLC is performing much quicker responsive compared to PD. FLC achieved the desired position under a one-second time frame as in Figure 34. Even though the simulation was start close to the upper saturation limit there are no overshooting or undershooting in both controllers.

To get the same steady-state error view as in the lower saturation start, needed to extend the view at the five-second mark. The extended view for the steady-state error is plotted in Figure 35.
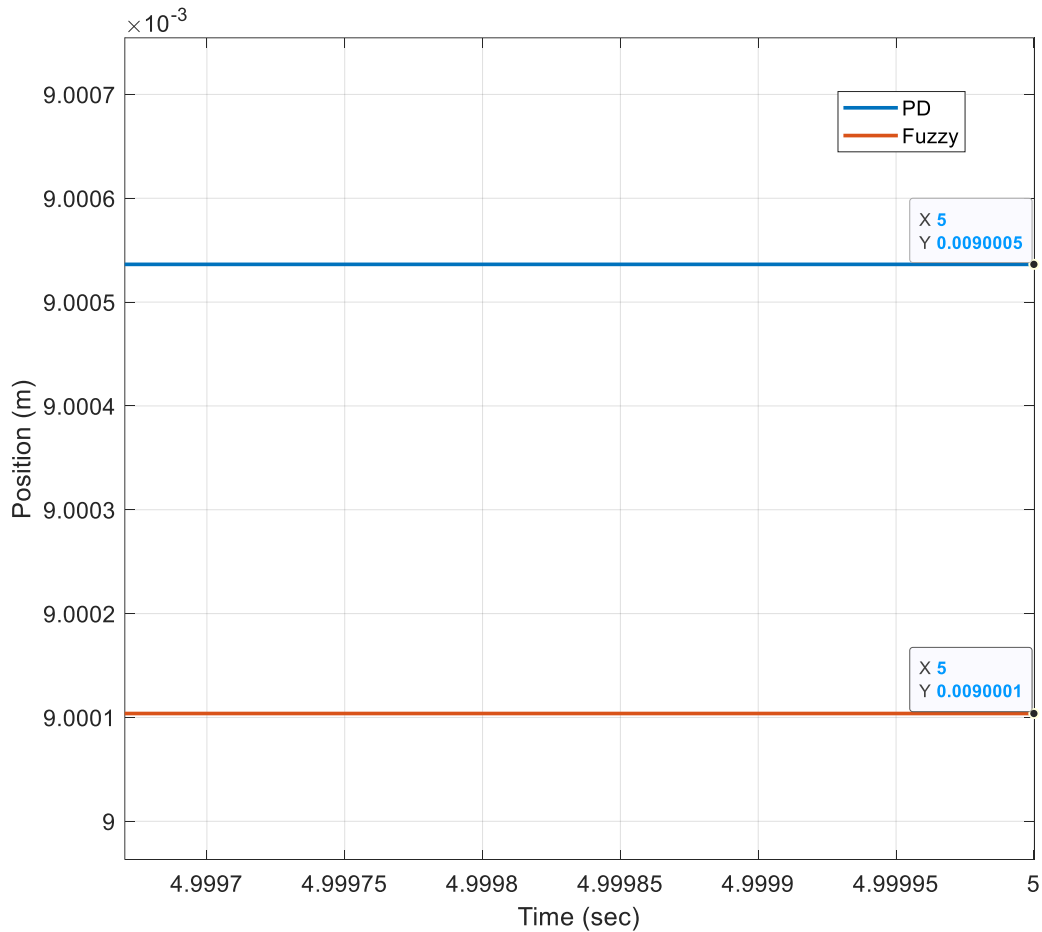
Figure 35. Steady-state error for PD vs Fuzzy starting from $1,9 \cdot 10^{-2}$ m

As shown in Figure 35 when the simulation started from a higher saturation limit FLC has a steady-state error of $1 \cdot 10^{-7}$ m compared to the PD value of $5 \cdot 10^{-7}$ m. Similarly, the simulation was run for a longer period to prove these values does not change over time. Hence the FLC has a better control effect compared to PD.

Compared to position parameter velocity also needs to meet certain criteria to be able to control the system. When the actual position reached its desired position, velocity should only move in between the setpoint and minimize the amplitude and eventually become zero as shown in Figure 36.
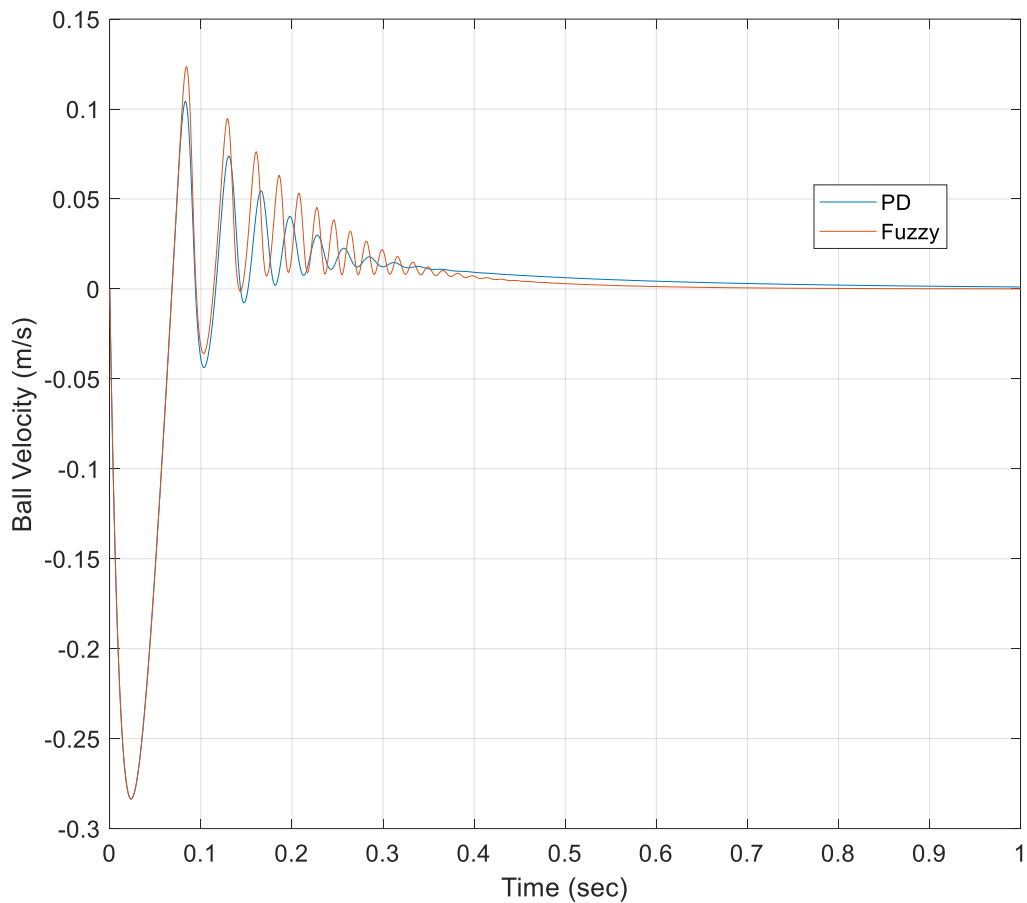
Figure 36. Velocity parameter for PD vs Fuzzy starting from $2 \cdot 10^{-4}$ m

Because the initial starting point is $2 \cdot 10^{-4}$ m which is marginally close to the upper magnet when the sphere is reaching its desired position it has some amount of velocity. This is the reason for the unstable behaviour around the set point for the sphere as seen in Figure 36. But when considering both controllers, Fuzzy have more amplitude while reaching the set point. Also, FLC reaches the required control value of zero sooner than the PD controller making it the better performing out of the two.

The same velocity parameter was plotted for the initial start at $1,9 \cdot 10^{-2}$ m as shown in Figure 37. The reason being for the much-stabilized system compared to Figure 36 is the sphere is moving upward direction toward the setpoint. Since the sphere is going against gravity no overshooting or undershooting can be seen on the velocity parameter.
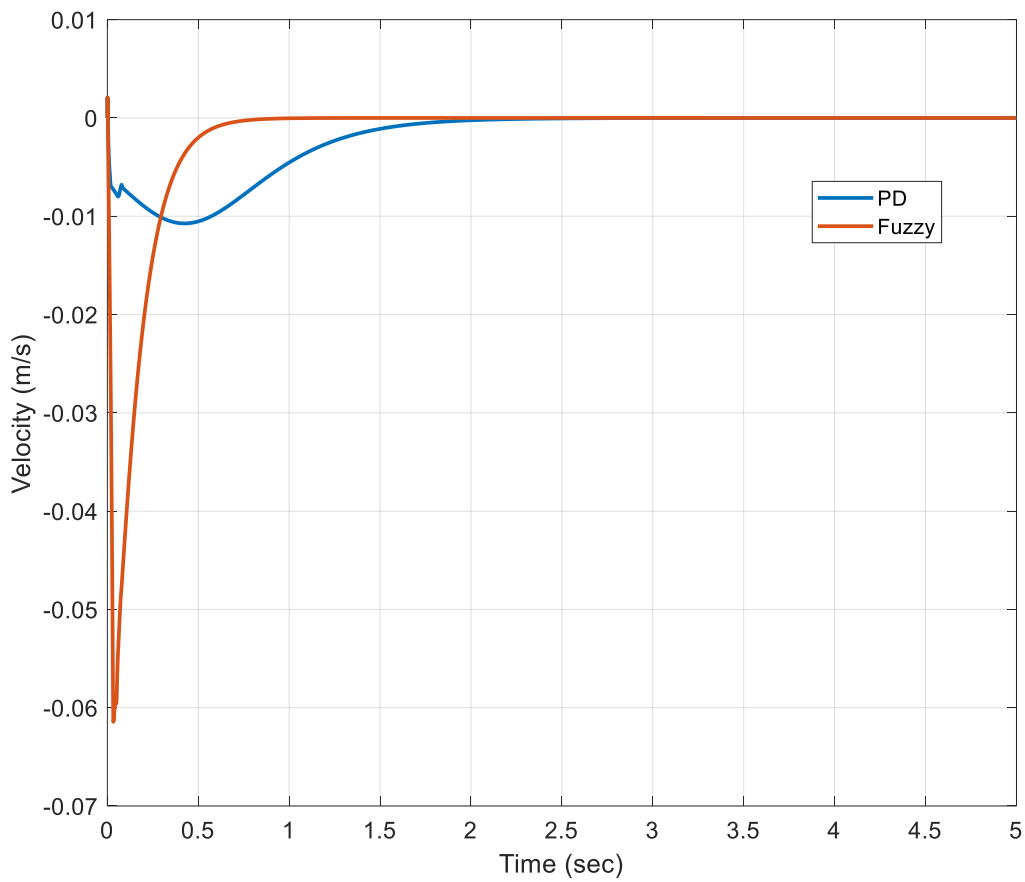
Figure 37. Velocity parameter for PD vs Fuzzy starting from $1{,}9 \cdot 10^{-2}$ m

Even though, comparing both position parameters results FLC is much quicker responsive compared to PD which took more than two seconds to acquire the desired position. The main reason due to quick responsiveness is FLC is moving through regions much quicker where PD is adjusting its behaviour as it goes on. When comparing Figure 36 vs Figure 37, the velocity is reaching zero much quicker in initial start $2 \cdot 10^{-4}$ m. The reason is the sphere is moving with gravity is much quicker compared to moving against it.

To get wider contrast regarding why FLC is quick responsive than PD need to consider the behaviour of the coil current parameter. From chapter 3.3 we conclusively proved, to achieve the desired position of $9 \cdot 10^{-3}$ m the needed current running through the coil is 0,9345 A. The value was achieved by both controller types as shown in Figure 38. The initial starting point was kept at $2 \cdot 10^{-4}$ m.

60
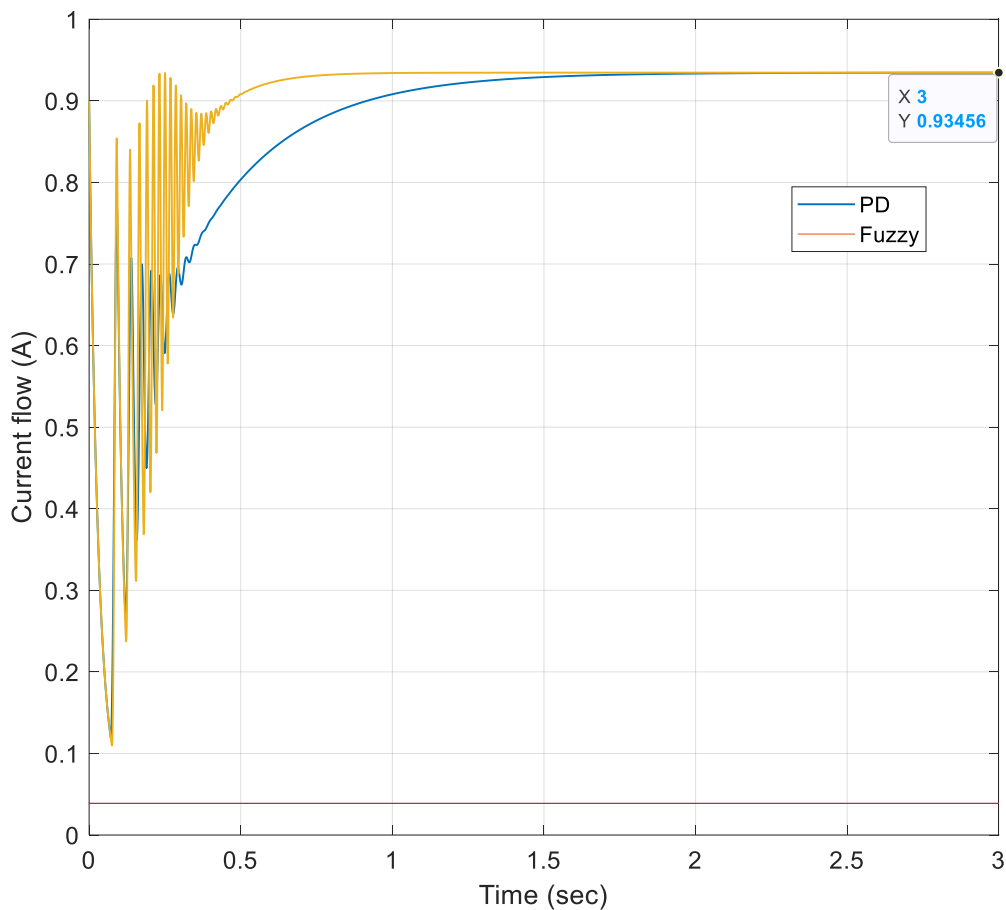
Figure 38. Coil current parameter for PD vs Fuzzy starting from 2·10⁻⁴ m

The simulation was taken for three seconds to get a much more clearer idea regarding the initial behaviour of the two controllers. When comparing the two controllers as in Figure 38, FLC reaches higher amplitudes in the early stages to move between the ranges faster and reaches the desired coil current value of 0,9345 A before the PD controller. The current change is co-related with the change of error resulting in similar graph patterns. Similar to the velocity parameter the coil current parameter is also having fluctuating behaviour due to the initial starting point which happens due to gravity. The rapid movement helps to keep a constant behaviour in the position parameter making it much more stable.

When the initial starting point changes to 1,9·10⁻² m, the behaviour is much more stable for the coil current parameter as shown in Figure 39. The reason being is the sphere is starting from closer to the lower magnet and goes upwards to reach the desired position.
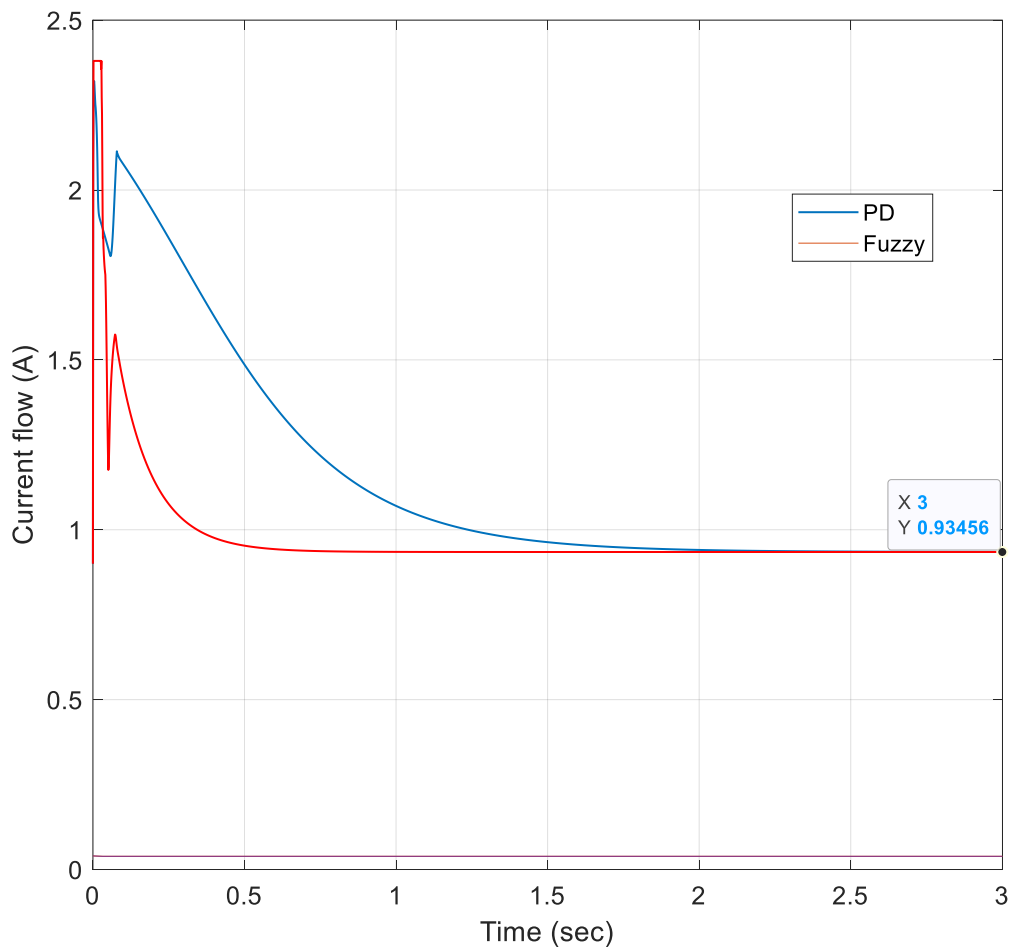
Figure 39. Coil current parameter for PD vs Fuzzy starting from $1,9 \cdot 10^{-2}$ m

In this scenario as well the FLC reaches the desired coil current value of 0,9345 A much faster than the PD controller. By the three-second mark, both of them reach the same value which can be seen in Figure 39. Coil current parameter was also plotted for ten seconds for both situations but the initial part was only plotted because from the three-second mark to the ten-second mark nothing will be changed other than maintaining the shown values on the plots.

Figure 39 clearly shows that energy consumption with a fuzzy controller is lower than PD, which this energy consumption can be important for the long-term operation of the system by changing the reference signals or disturbing it.

Considering the control parameter, the behaviour is very similar to the coil current behaviour. The reason being the control parameter's main objective is to give the coil current relevant amount of current fluctuations to reach the desired value. For the initial start of $2 \cdot 10^{-4}$ m, control parameter behaviour can be plotted as Figure 40.
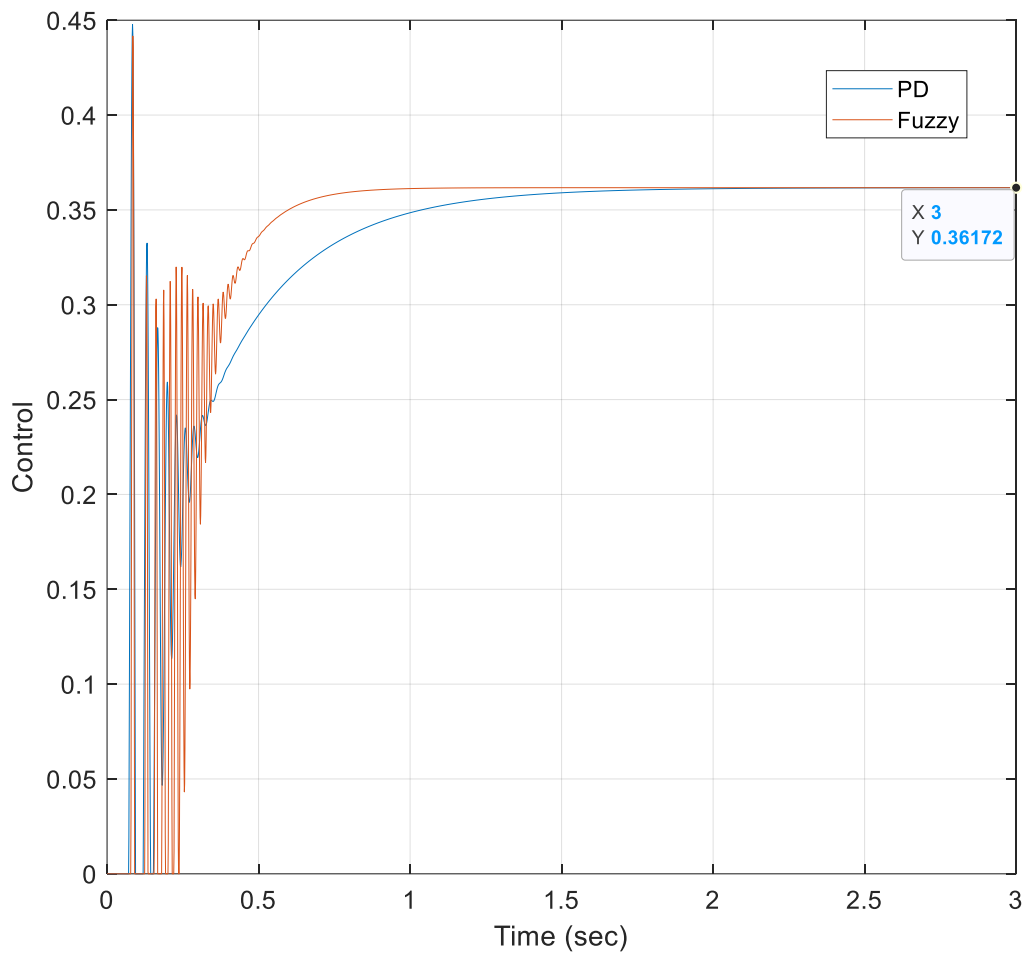
Figure 40. Control PWM signal for PD vs Fuzzy starting from $2 \cdot 10^{-4}$ m

When evaluating the PD control behaviour it does not have a lot of amplitude fluctuations at the initial part. Because PD control tends to adjust its control as time goes on. But meanwhile, FLC has bigger amplitude fluctuations as seen in Figure 40 and tend to reach the control level of 0,3617 much quicker compared to PD. The reason for the quick changes are the higher value of change of error compared to the PD and also sphere is going downwards with the gravity.

Similarly, by changing the initial starting point to $1,9 \cdot 10^{-2}$ m both of the controllers have no fluctuations as seen in Figure 41 since the sphere is moving upward towards its desired position.
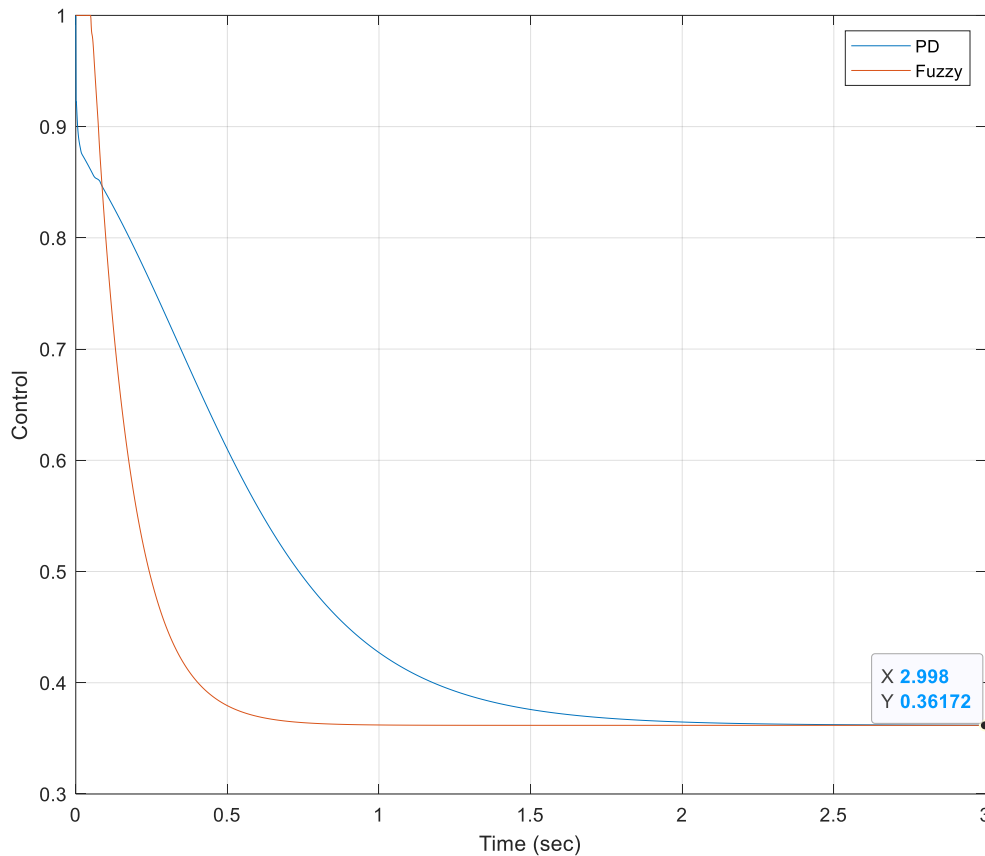
Figure 41. Control PWM signal for PD vs Fuzzy starting from $1,9 \cdot 10^{-2}$ m

Both controllers start from a higher control value since the sphere needs to move upwards against gravity. This is the same reason for higher current values at the beginning in Figure 39. But as the sphere is reaching its desired position the control value also decreases and maintains the value of 0,3617. But comparatively, FLC is reaching that limit much rapidly under one second while PD controller is taking more than two seconds to reach the same value.

Finally, the FLC was connected to the actual system and the results were obtained as in Figure 42. The platform which holds the ball was removed in this process to observe the pulse excitation. For the first instance, the EM2 value was set to value zero as in Figure 30 from the manual switch and the model was built and it was run.
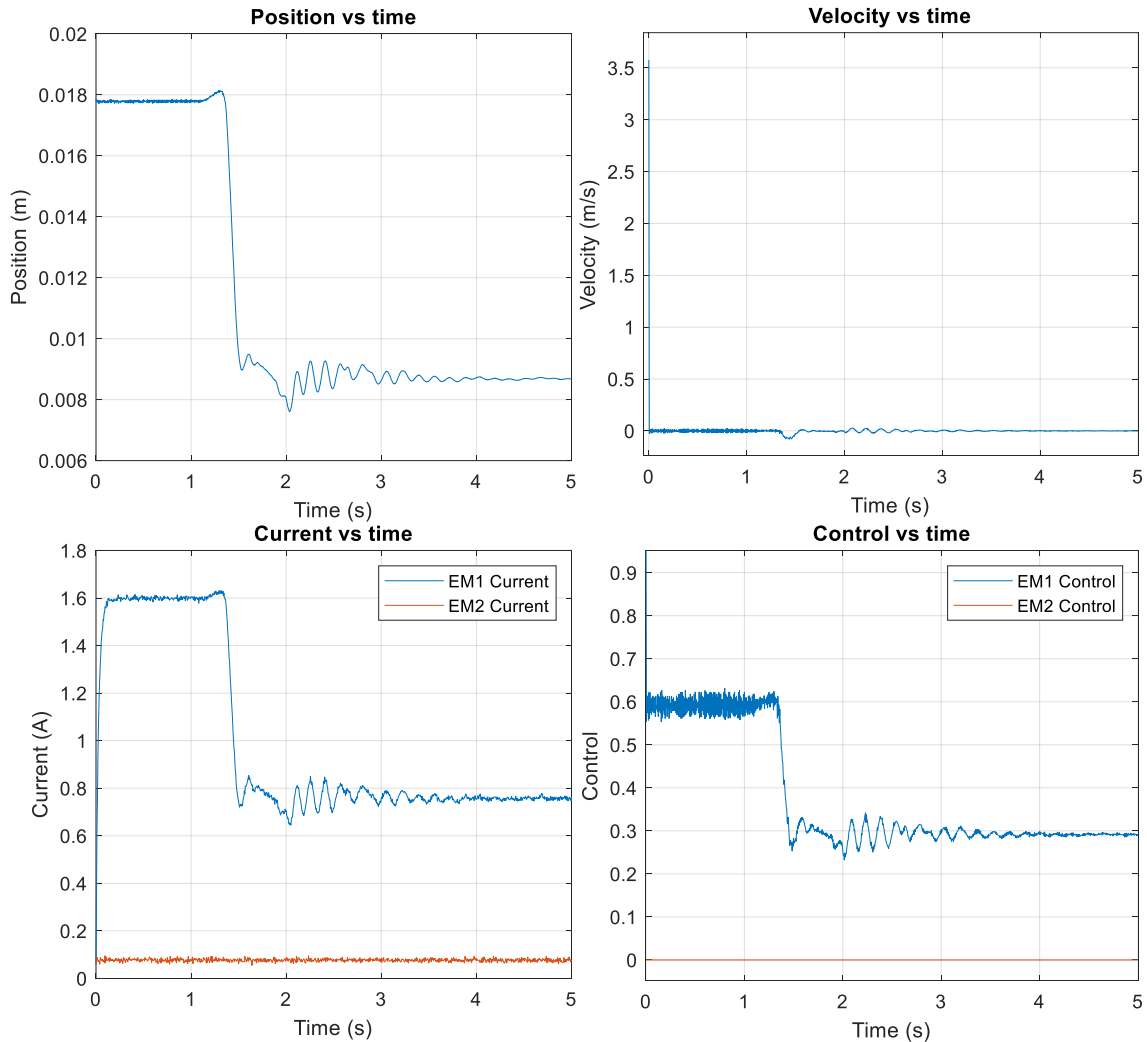
Figure 42. Parameters for the actual system run with EM2=0

After running the model the sphere was held next to the magnets so it will reach the set point. The initial disturbance is resulting due to placing the sphere in the operating range and after that when the sphere is at the setpoint it maintains the desired value of $9 \cdot 10^{-3}$ m. And the velocity is zero in this giving instance making the system a perfectly balanced control system. Since the actual ball was less heavy than the simulated ball the desired coil current to keep the metallic sphere in place is lower than the simulated value of 0,9345 A. Since EM2 is zero the model run was constant for the twenty-second runtime.

Next, the EM2 was changed from zero to pulse excitation range with an amplitude of 0,2. Then the model was built and it was run for twenty seconds. The parameter behaviour for the pulse excitation stage can be seen in Figure 43.
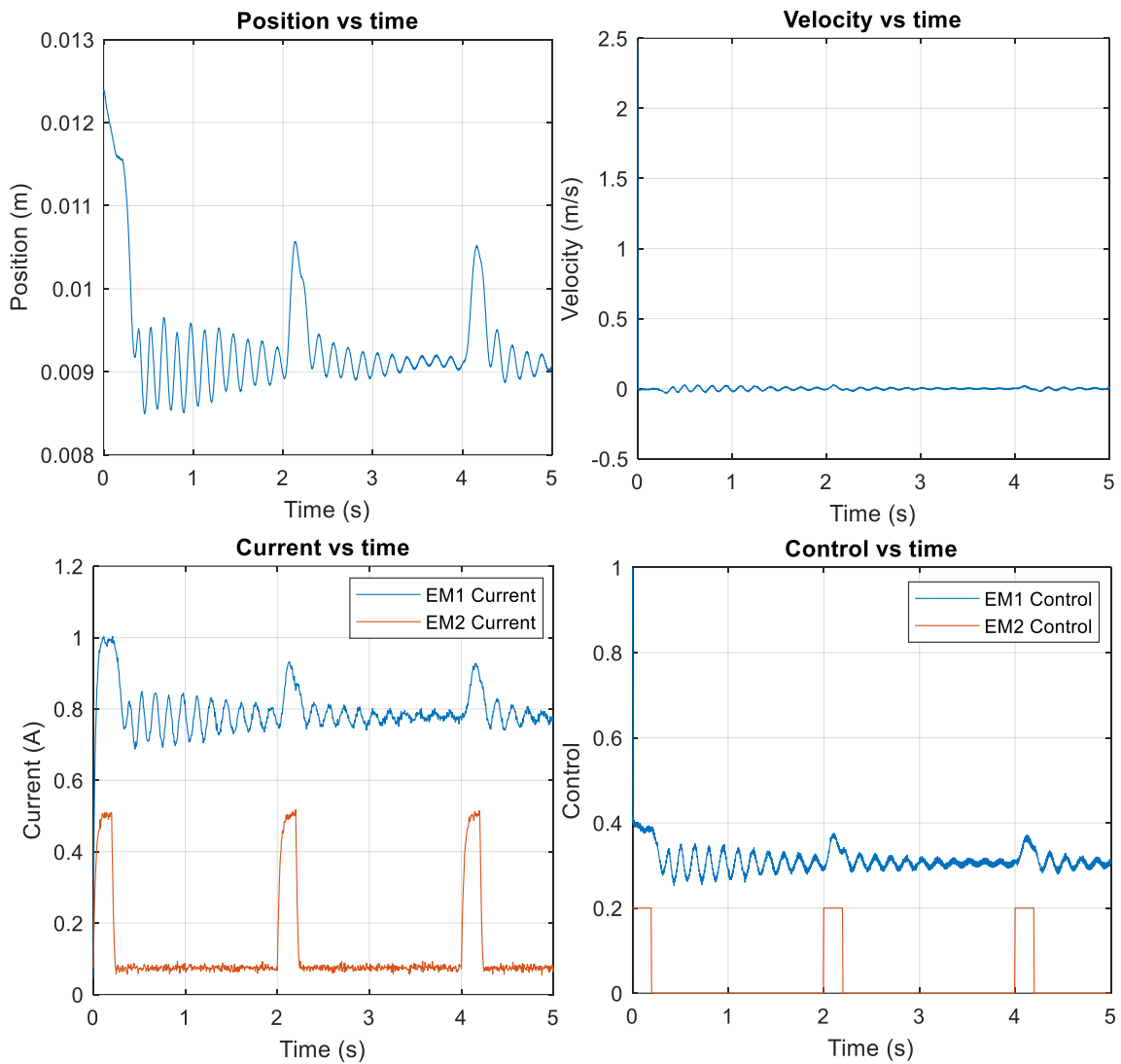
Figure 43. Parameters for the actual system run with pulse excitation

When the system was given with the pulse excitation, the position parameter both graphically and physically moved downwards from the given setpoint. The small motion downwards does not reflect highly on the position parameter since the velocity of going downwards and coming back to the setpoint is very trivial compared to the other parameters. But it does fluctuate both ways from the value zero. Clear evidence of the pulse behaviour can be seen on the coil current parameter. The orange line denotes the pulse response happening in the lower EM2.

At the peak point close to 0,5 A is generating in the lower magnet and to compensate for that behaviour, upper EM1 is also increasing the coil current as seen on the blue line in Figure 43.

Similar behaviour can be seen on the control parameter as well to mitigate the sphere from going out of the control range. As an experimental purpose, the pulse amplitude was doubled and the sphere went out of the operating range as a result. The goal of the research thesis was achieved by getting both simulation results and actual model results.

SUMMARY

The main intention work behind the thesis is to develop a better controller alternative for the PD controller in the MLS2EM system which was built by Inteco. The MLS2EM control system is situated and the experiment was conducted in Alpha Control Laboratory in Taltech. The development process begins by understanding how the default controller works and implying it from a different perspective of view.

In the background of the literature review, there have been a lot of alternative controller options have been discussed. The essential requirement for replacing the controller is PD controllers in general not suitable for highly non-linear systems. But FLC is suitable for both linear and non-linear control systems. This is the main reason behind choosing a fuzzy controller over other methods. FLC tends to have more robust control and quicker responsiveness compared to PD controllers. With PD controllers, to get the optimal response parameters the controller needs to be properly tuned and this task can be complex and time-consuming. But with FLC after the design process only minimal changes needed to be done to optimize the control system.

The goal was to replace the PD, not with a similar type of performance but better much faster responsive less steady-state error and much more stable in the actual system. To achieve much more smooth control the membership plots for each input needed to increase from three at the beginning to five for better performance. As a result total rules were also increased from nine to twenty-five giving relatively lots of arguments and logical connections for the control system. FLC also have better steady-state error results as well compared to the PD reaching the same as the desired value with only an infinitesimal error which is five times smaller than the PD controller.

Since the MLS2EM system only requires two inputs PD controller can be used but if the inputs are higher or outputs are higher PD cannot be used in these cases. In terms of multiple inputs or outputs with proper logical connections, FLC can be used. For smaller less complex systems with smaller control ranges preferably can use PD controllers instead of FLC. To improve the actual control system and operating range needed to install better position sensor mechanics and wider frames to allow the sphere to be able to get more travelling distances. In this case, both electromagnets should be much more powerful as well.

In conclusion, when using FLC instead of other controller types it has a better changeability and manoeuvrability depending on the control environment and the rules

applied to it. With FLC it is really important to get the operating range and the correct logical rules in that range.

As a result of knowing the ranges and how the membership plots are changing development of the current FLC can be increased by improving the number of membership plots. But the plots needed to be increased with odd numbers so there will be always a plot representing the centre region with uniform distribution. For the next step if the membership plots were increased to seven the result will be a control system with 49 rules. This was extremely important and interesting to understand how the FLC is working and how to implement it at an industrial level.

KOKKUVÕTE

Lõputöö peamine eesmärk on töötada välja Inteco poolt ehitatud MLS2EM süsteemis PD-kontrolleri jaoks parem kontrolleri alternatiiv. MLS2EM juhtimissüsteem asub ja katse viidi läbi Taltechi Alpha Control Laboratory'is. Arendusprotsess algab vaikekontrolleri tööpõhimõtte mõistmisest ja selle vihjamisest erinevast vaatenurgast. Kirjanduse ülevaate taustal on arutatud palju alternatiivseid kontrolleri võimalusi. Kontrolleri asendamise põhinõue on PD-kontrollerid, mis üldiselt ei sobi väga mittelineaarsete süsteemide jaoks. Kuid FLC sobib nii lineaarsete kui ka mittelineaarsete juhtimissüsteemide jaoks. See on peamine põhjus, miks valite muude meetodite asemel häguse kontrolleri. FLC-l on PD-kontrolleritega võrreldes tugevam juhtimine ja kiirem reageerimisvõime. PD-kontrollerite puhul tuleb optimaalsete reaktsiooniparameetrite saamiseks kontroller korralikult häälestada ning see ülesanne võib olla keeruline ja aeganõudev. Kuid FLC puhul tuli pärast projekteerimisprotsessi juhtimissüsteemi optimeerimiseks teha vaid minimaalseid muudatusi.

Eesmärk oli asendada PD, mitte sarnast tüüpi jõudlusega, vaid paremini palju kiiremini reageeriva, vähem püsiva oleku veaga ja tegelikus süsteemis palju stabiilsem. Palju sujuvama juhtimise saavutamiseks tuli parema jõudluse huvides suurendada iga sisendi liikmesusgraafikuid alguses kolmelt viiele. Selle tulemusena suurendati ka reeglite koguarvu üheksalt kahekümne viiele, mis annab juhtimissüsteemi jaoks suhteliselt palju argumente ja loogilisi seoseid. FLC-l on ka paremad püsiseisundi veatulemused, võrreldes PD-ga, mis saavutab soovitud väärtuse, vaid lõpmatu väikese veaga, mis on viis korda väiksem kui PD-kontrolleril.

Kuna MLS2EM süsteem vajab ainult kahte sisendit, saab kasutada PD-kontrollerit, kuid kui sisendid on suuremad või väljundid on suuremad, ei saa PD-d sellistel juhtudel kasutada. Mitme õige loogilise ühendusega sisendi või väljundi puhul saab kasutada FLC-d. Väiksemate ja väiksemate juhtimisvahemikega, vähem keerukate süsteemide puhul võib FLC asemel eelistatavalt kasutada PD-kontrollereid. Tegeliku juhtimissüsteemi ja töövahemiku parandamiseks on vaja paigaldada parem asendianduri mehaanika ja laiemad raamid, et kera saaks läbida rohkem vahemaid. Sel juhul peaksid mõlemad elektromagnetid olema ka palju võimsamad.

Kokkuvõtteks võib öelda, et kui kasutada FLC-d teiste kontrolleritüüpide asemel, on sellel parem muudetavus ja manööverdusvõime sõltuvalt juhtimiskeskkonnast ja sellele rakendatavatest reeglitest. FLC-ga on tõesti oluline saada töövahemik ja õiged loogilised reeglid selles vahemikus.

Teades vahemikke ja seda, kuidas liikmeskonnaplaanid muutuvad, saab praeguse FLC arengut suurendada liikmeskondade arvu parandamise teel. Kuid proovitükke tuli suurendada paaritute arvudega, nii et alati oleks graafik, mis esindab ühtlase jaotusega keskpiirkonda. Järgmise sammuna, kui liikmete arv suurendati seitsmeni, on tulemuseks 49 reegliga kontrollsüsteem. See oli äärmiselt oluline ja huvitav, et mõista, kuidas FLC töötab ja kuidas seda tööstuslikul tasandil rakendada.

REFERENCES

[1]   C. M. Lin, M. H. Lin, and C. W. Chen, "SoPC-based adaptive PID control system design for magnetic levitation system," *IEEE Syst. J.*, vol. 5, no. 2, pp. 278–287, 2011, doi: 10.1109/JSYST.2011.2134530.

[2]   T. Morita, K. Shimizu, M. Hasegawa, K. Oka, and T. Higuchi, "A miniaturized levitation system with motion control using a piezoelectric actuator," *IEEE Trans. Control Syst. Technol.*, vol. 10, no. 5, pp. 666–670, 2002, doi: 10.1109/TCST.2002.801802.

[3]   K. H. Lundberg, K. A. Lilienkamp, and G. Marsden, "Low-Cost Magnetic Levitation Project Kits," *IEEE Control Syst.*, vol. 24, no. 5, pp. 65–69, 2004, doi: 10.1109/MCS.2004.1337863.

[4]   Y.-S. Shiao, "Design and Implementation of a Controller for a Magnetic Levitation System," *Proc. Natl. Sci. Counc. ROC(D)*, vol. 11, no. 2, pp. 88–94, 2001.

[5]   P. Balko and D. Rosinova, "Modeling of magnetic levitation system," *Proc. 2017 21st Int. Conf. Process Control. PC 2017*, pp. 252–257, 2017, doi: 10.1109/PC.2017.7976222.

[6]   C. Dragos, M. Radac, and R. Precup "Gain-Scheduling Control Solutions for MLS"

[7]   Magnetic Levitation System 2EM (MLS2EM), USB Version, User's manual

[8]   I. Ahmad and M. Javaid ," Nonlinear Model & Controller Design for MLS"

[9]   K. Kecik, A. Mitura, S. Lenci, and J. Warminski, "Energy harvesting from a magnetic levitation system," *Int. J. Non. Linear. Mech.*, vol. 94, no. June 2016, pp. 200–206, 2017, doi: 10.1016/j.ijnonlinmec.2017.03.021.

[10]   E. Hedrea, "TP – Based Fuzzy Control Solutions for Magnetic Levitation Systems," pp. 809–814, 2019.

[11]   Y. W. Bai and C. F. Lee, "Magnetic Levitation Wireless Charging Platform with Adjustable Magnetic Levitation Height and Resonant Frequency for a Better Charging Efficiency," *2018 IEEE 7th Glob. Conf. Consum. Electron. GCCE 2018*, pp. 712–713, 2018, doi: 10.1109/GCCE.2018.8574495.

[12]   J. H. Jeong, C. W. Ha, J. Lim, and J. Y. Choi, "Analysis and Control of the Electromagnetic Coupling Effect of the Levitation and Guidance Systems for a Semi-High-Speed MAGLEV Using a Magnetic Equivalent Circuit," *IEEE Trans. Magn.*, vol. 52, no. 7, pp. 52–55, 2016, doi: 10.1109/TMAG.2015.2506681.

[13] J. H. Jeong, C. W. Ha, J. Lim, and J. Y. Choi, "Analysis and Control of Electromagnetic Coupling Effect of Levitation and Guidance Systems for Semi-High-Speed Maglev Train Considering Current Direction," *IEEE Trans. Magn.*, vol. 53, no. 6, p. 2021, 2017, doi: 10.1109/TMAG.2017.2659703.

[14] C. Zhang, Y. Jing, J. Kong, T. Peng, Z. Liao, and J. Hao, "Method for Measuring Levitation Gap of Magnetic Levitation Ball Based on Image Processin," *Proc. 2019 3rd IEEE Int. Conf. Robot. Autom. Sci. ICRAS 2019*, pp. 215–219, 2019, doi: 10.1109/ICRAS.2019.8808955.

[15] A. M. Benomair and M. O. Tokhi, "Control of single axis magnetic levitation system using fuzzy logic control," *Proc. 2015 Sci. Inf. Conf. SAI 2015*, pp. 514–518, 2015, doi: 10.1109/SAI.2015.7237191.

[16] D. Suman and R. Bhatt, "Robust I-fuzzy controller for magnetic ball levitation," *Proc. Int. Conf. Electron. Commun. Aerosp. Technol. ICECA 2017*, vol. 2017-January, no. 1, pp. 618–621, 2017, doi: 10.1109/ICECA.2017.8203612 [16]

[17] J. Zhang *et al.*, "Torque optimization of a novel reaction sphere actuator based on support vector machines," *Proc. 4th IEEE Int. Conf. Appl. Syst. Innov. 2018, ICASI 2018*, pp. 263–266, 2018, doi: 10.1109/ICASI.2018.8394583.

[18] G. Qi and Z. Wu, "Filter-based tracking of magnetic levitation ball system," *Proc. 30th Chinese Control Decis. Conf. CCDC 2018*, pp. 3135–3139, 2018, doi: 10.1109/CCDC.2018.8407663.

[19] M. J. Khan and M. Junaid, "Modelling , Simulation & Control of Non-Linear Magnetic Levitation System," 2018.

[20] X. J. Shao, F. Bin Meng, Z. M. Chen, and Q. S. He, "The exponential reaching law sliding mode control of magnetic levitation system," *Proc. 28th Chinese Control Decis. Conf. CCDC 2016*, no. 20132050, pp. 3500–3503, 2016, doi: 10.1109/CCDC.2016.7531588.

[21] J. Zhang, X. Wang, and X. Shao, "Design and Real-Time Implementation of Takagi-Sugeno Fuzzy Controller for Magnetic Levitation Ball System," *IEEE Access*, vol. 8, pp. 38221–38228, 2020, doi: 10.1109/ACCESS.2020.2971631.

[22] K. Anurag and S. Kamlu, "Design of LQR-PID controller for linearized magnetic levitation system," *Proc. 2nd Int. Conf. Inven. Syst. Control. ICISC 2018,* no. Icisc, pp. 444–447, 2018, doi: 10.1109/ICISC.2018.8399112.

[23] J. E. Goff, "Heuristic model of air drag on a sphere," *Phys. Educ.*, vol. 39, no. 6,

pp. 496–499, 2004, doi: 10.1088/0031-9120/39/6/005.

[24] J. Almedeij, "Drag coefficient of flow around a sphere: Matching asymptotically the wide trend," *Powder Technol.*, vol. 186, no. 3, pp. 218–223, 2008, doi: 10.1016/j.powtec.2007.12.006.

[25] D. Viviantoro, A. Zuhdi, A. Purbhadi, and Mujamilah, "Thermal Effect on Electromagnetic Suspension for Air Gap Performance in Magnetic Levitation System," *J. Phys. Conf. Ser.*, vol. 1204, no. 1, 2019, doi: 10.1088/1742-6596/1204/1/012059.

[26] D. . Shu'aibu, H. Rabiu, and N. Shehu, "Efficient fuzzy logic controller for magnetic levitation systems," *Niger. J. Technol. Dev.*, vol. 13, no. 2, p. 50, 2017, doi: 10.4314/njtd.v13i2.2.

[27] E. L. Hedrea, R. E. Precup, R. C. Roman, and E. M. Petriu, "Tensor product-based model transformation approach to tower crane systems modeling," *Asian J. Control*, vol. 23, no. 3, pp. 1313–1323, 2021, doi: 10.1002/asjc.2494.